

A Survey on Magnetic Resonant Coupling Wireless Power Transfer Technology for Electric Vehicle Charging

Xiaolin Mou¹, Daniel T. Gladwin^{2*}, Rui Zhao³, and Hongjian Sun⁴

¹ Department of Electronic and Electrical Engineering, The University of Sheffield, Sheffield, United Kingdom

² Department of Electronic and Electrical Engineering, The University of Sheffield, Sheffield, United Kingdom

³ Department of Electronic and Electrical Engineering, The University of Sheffield, Sheffield, United Kingdom

⁴ Department of Engineering, Durham University, Durham, United Kingdom

* E-mail: d.gladwin@sheffield.ac.uk

Abstract: Wireless Power Transfer technology (WPT) makes it possible to supply power through an air-gap, without the need for current-carrying wires. One important technique of WPT technology is magnetic resonant coupling (MRC) WPT. Based on the advantages of MRC WPT, such as safety and high power transfer efficiency over a long transmit distance, there are many possible applications of MRC WPT. This paper provides a comprehensive, state-of-the-art review of the MRC WPT technology and wireless charging for electric vehicle (EV). A comparative overview of MRC WPT system design which includes a detailed description of the prototypes, schematics, compensation circuit topologies (impedance matching), and international charging standards. In addition, this paper provides an overview of wireless EV charging including the static wireless EV charging and the dynamic wireless EV charging, which focuses on the coil design, power transfer efficiency, and current research achievement in literature.

1 Introduction

The increasing requirement for convenience and safety has prompted an ever-growing demand for wireless charging, and with increasing efforts devoted to the development of electronic based technologies, such as mobile phones and electric vehicles (EVs), we are now able to enjoy the benefit of wireless charging.

WPT technologies can be categorized in different ways. One method for classifying WPT technologies depends on the range of power delivery: far-field WPT technology and near-field WPT technology. Far-field WPT technology is based on the electro-magnetic radiation technique, using the microwave, laser or solar satellite. Near-field WPT technology includes capacitive coupling WPT (CPT) and inductive coupling WPT (Inductive power transfer (IPT) and magnetic resonant coupling (MRC) WPT). The major difference between IPT and MRC is: MRC WPT is very effective for low- or medium -power WPT and the primary and secondary coils are tuned in resonant frequency by adding compensation capacitors; IPT WPT is better for high-voltage power transfer since there is no resonant circuit involved. Use of MRC WPT is advantageous with respect to its high safety and long transmission distance. Fig. 1 shows a comparison of IPT WPT and MRC WPT [1].

Wireless charging technology for EVs could save the consumer from the laborious process of finding a charging point, connecting up the cable and time spent waiting for the charge to complete, on the assumption that the cable is neither lost or broken. Wireless EV charging can be either static or dynamic, based on the mobility of the charging facility. Static wireless charging technology may refer to the case where the charging ports are installed in the parking area, while dynamic wireless charging technology could be more flexible, the EVs can be powered while driving, even saving the trouble of installing additional batteries if the energy source is on the path. MRC WPT technology is one useful technique for EVs charging design. The advantages of MRC wireless EV charging include a high transmission efficiency with a long gap distance (more than 100 mm).

This paper reviews the MRC WPT technology and the wireless EV charging application. This paper is organised as follows. Section

II discusses the design of the MRC WPT system, including prototypes, schematics, compensation circuit topologies, and international charging standards. Section III reviews wireless EV charging systems based on the MRC technique. The conclusion is in Section IV.

2 MRC WPT System Design

Many different schemes have been proposed for MRC WPT wireless charging systems. This section focuses on introducing the details of MRC WPT system design which includes prototypes, schematics, compensation circuits, and several international charging standards.

2.1 The Prototypes of MRC System

The performance of MRC WPT system varies with different prototypes of the design. According to the number of transmitters, MRC WPT systems can be classed as either single-input-single-output (SISO), single-input-multiple-output (SIMO), multiple-input-single-output (MISO), or multiple-input-multiple-output (MIMO). Fig. 2 shows the difference between these four prototypes.

2.1.1 SISO and SIMO Prototype: The SISO WPT is the most basic and simple prototype of the WPT systems. In a SISO WPT system, the receiver load plays an important role in the transfer function of the system. Moreover, the distance and orientation of the coils greatly affect the reflected load impedance on the transmitter side. In a MISO WPT system, due to the cross-coupling between the different transmitters, the effects of the load upon the transfer function and efficiency of the system are increased.

H.D.Lang *et al.* [2] present a comparison between the MISO and SISO. The multi-transmitter WPT systems have several advantages over their single-transmitter counterparts, most importantly higher power transfer efficiency (PTE). Because of the higher PTE, the magnetic field strength required to transfer a particular amount of power is also lower for a MISO WPT system compared to their SISO counterpart, and less magnetic field intensity can reduce the harm of human body. The MISO WPT system is a viable candidate for biomedical implants and general purpose electronics.

	IPT WPT (No-resonant Coupling)	MRC WPT (Resonant Coupling)
Circuit Model		
Equivalent impedance Z	$Z = R_1 + j\omega L_1 + \frac{k^2 \omega^2 L_1 L_2}{j\omega L_2 + R_2 + R_{Load}}$	$Z = R_1 + \frac{k^2 \omega^2 L_1 L_2}{R_2 + R_{Load}}$
Advantages	Simple, safe, and high transfer efficiency in short transmission distance.	Longer transmission distance than inductive WPT.
Disadvantages	Short transmission distance.	Difficult to adjust resonant frequency for multiple devices.

Fig. 1: A comparison of IPT WPT and MRC WPT [1]

SISO Prototype		MISO Prototype	
<ul style="list-style-type: none"> • Basic system prototype; • Simple design. 	<ul style="list-style-type: none"> • Comparing with SISO, Higher transfer efficiency; • Less magnetic field intensity to human. 	SIMO Prototype	MIMO Prototype
		<ul style="list-style-type: none"> • Apply to Multiple devices charge 	<ul style="list-style-type: none"> • Apply to Electromagnetic radiation WPT; • Multiple device charging case.

Fig. 2: Comparison of SISO, SIMO, MISO and MIMO

2.1.2 MISO Prototype: Elisenda *et al.* [3] provide a design-oriented model-based scalability analysis of a SIMO WPT system. The scalability and behavior of a SIMO system strongly depends on how the coupling between the transmitter and the receivers, and the coupling between receivers, scale when the number of nodes is increased. There are two key scenarios which entail different couplings between the system nodes:

1. Increase Density: when the number of receivers is increased within a constrained area. The coupling between the transmitter and the receivers is maintained but the coupling between the receivers is

increased due to their reduced separation. In this case, the point-to-point efficiency decreases when the number of nodes increase and the system efficiency increases. The output power is not increased when the number of receivers is increased, which can be explained by the fact that the over-coupling of the system is increased when the number of receivers is increased.

2. Constant Density: when the number of receivers is increased together with the deployment area, the coupling between transmitter and receivers is decreased but the coupling between receivers is maintained because the density remains constant. In this case, power efficiency and output power varies when the number of receivers is

increased. However, the system can achieve maximum output power and system efficiency with an optimal number of receivers.

2.1.3 MIMO Prototype: MIMO systems are always used in electromagnetic radiation WPT applications [4–6], *e.g.*, wireless sensor networks. The exact resonant frequency between the transmitter and receiver is necessary, so the MIMO systems are not widely used in MRC WPT technology. However, H. Sun *et al.* [7] propose an algorithm which can maximize the power of the intended receiver device while limiting the power received by the unintended device. The numerical results show that the algorithm can significantly improve the power efficiency. One important result of the MIMO system observes that even though all the nodes have the same resonant frequency, the maximum point-to-point efficiency is not obtained at this frequency, since all the receivers are coupled between them, and the system presents an over-coupled regime response. For wireless electric vehicle charging technology, the SISO and MISO system are the best systems to use.

2.2 The Schematics of the MRC WPT System:

In previous research, a typical MRC WPT system is generally classified as either a two-coil or a four-coil system. Fig. 3 **2-Coil** shows the two-coil MRC WPT system. The two-coil MRC WPT system consists of two electromagnetic subsystems with the same natural resonant frequency, and it is the original type of the SISO MRC WPT system. To improve PTE at longer transmission distances, the four-coil system has been proposed. Fig. 3 **4-Coil** shows the four-coil MRC WPT system. In this system, the transmitter includes a source coil and a sending coil (or primary coil), the receiver includes a receiving coil (or secondary coil) and a load coil.

A conventional four-coil system [8–10] offers the advantage of two degrees of freedom such that the source coil can be mounted and coupled with the sending coil to adjust the system input impedance, and the load coil can be mounted and coupled with the receiving coil to adjust the equivalent load resistance from the receiving coil to match the load condition. A conventional four-coil system is suitable for mid-range applications while a two-coil system gives better performance in short-range applications. Applications are considered short-range or mid-range based on whether the transmission distance is smaller or larger than the coil dimension. *e.g.*, in electric vehicle (EV) applications, the transmission distance, also known as air-gap, ranges typically from 100 mm to 300 mm, and the coil dimension is always larger than the transmission distance. Therefore, a two-coil system is adopted for this short-range application.

S.Moon *et al.* [11] propose an asymmetric four-coil system, the primary side consists of a source coil and two transmitter coils which are called intermediate coils, and in the secondary side, a load coil serves as a receiver coil. The enhancement of the apparent coupling coefficient at the operating frequency is superior to the conventional four-coil system. Thus, the asymmetric four-coil system can reduce the number of turns in the source coil and the root mean square input current when compared to the conventional four-coil system and two-coil system. This asymmetric four-coil system has a higher PTE which enables a relatively long distance between the source coil and load coil.

PTE and power delivered to the load (PDL) are two key parameters in WPT technology, which affect the energy source specifications, heat dissipation, power transmission range, and interference with other devices. Despite the improvement of PTE at large transmission distance, the four-coil system causes a significant reduction in power delivered to load (PDL) [12]. M. Kiani *et al.* [12] and Y. Li *et al.* [13] propose a three-coil MRC WPT system, as shown in Fig. 3 **3-Coil**. This topology not only provides a PTE as high as the four-coil method but also offers a PDL that is significantly higher than the four-coil MRC WPT system at large transmission distance.

2.3 Compensation Circuit Topology of MRC WPT System:

The compensation circuit is often required for both transmitter and receiver in the MRC system to improve the power transfer capability. There are four basic compensation circuits and several hybrid compensation circuits in the MRC WPT system.

2.3.1 Basic Compensation Circuit: Apart from making the system resonant, the benefit of a compensation circuit includes minimising the volt-ampere (VA) rating of the power supply and regulating the value of current in the supply loop as well as the voltage of the receiving loop with higher efficiency. Four elemental compensation topologies can be summarised out of the existing literature: series-series (S-S) compensated, parallel-parallel (P-P) compensated, series-parallel (S-P) compensated and parallel-series (P-S) compensated, as shown in Fig. 4. The difference lies in the placement of compensation capacitors in terms of either in parallel or in series with the primary or secondary leakage inductance.

The process of choosing the compensation topology varies for primary and secondary sides based on the functionalities. In the primary side, the implementation of different topologies depends on the demanded transmission range or voltage in practical scenarios. For example, series compensation topology is sufficient for distance transmission, while parallel compensation is generally regarded as the optimal choice when the primary coil requires large current. In the secondary part, series compensation has voltage source characteristics, thus it is well suited for systems that have an intermediate DC bus. Meanwhile, parallel compensation has current source characteristics and is well suited for battery charging [14].

Normally, the resonant operating frequency for the basic compensation topology is:

$$\omega = \frac{1}{\sqrt{L_p C_p}} = \frac{1}{\sqrt{L_s C_s}} \quad (1)$$

The reflected impedance from the secondary to the primary can be expressed as:

$$Z_r = \frac{\omega^2 M^2}{Z_s} \quad (2)$$

The impedance of the primary side Z_p depends on the compensation topology, which can be expressed as [15]:

$$Z_p = j\omega L_p + \frac{1}{j\omega C_p} + Z_r(\text{series}) \quad (3)$$

$$Z_p = \frac{1}{j\omega C_p + \frac{1}{j\omega L_p + Z_r}}(\text{parallel}) \quad (4)$$

The impedance of the secondary side Z_s depends on the compensation topology, which can be expressed as:

$$Z_s = j\omega L_s + \frac{1}{j\omega C_s} + R(\text{series}) \quad (5)$$

$$Z_s = j\omega L_s + \frac{1}{j\omega C_s + \frac{1}{R}}(\text{parallel}) \quad (6)$$

The S-S topology compensation structure and P-S compensation structure have the highest transmission efficiency. In comparison, the S-S compensation structure is superior to the other three structures when the system is resonant, its load receiving power and system transmission efficiency are better, so the S-S topology is used in MRC WPT frequently [16]. Fig. 4 demonstrated a typical S-S compensation topology [17]. L_p refers to the transformer inductances on the primary side, while L_s indicates the one on the secondary side. Likewise, C_p and C_s refer to the primary and secondary compensation capacitors which are used for enhancing energy transferred

Name	Schematics	Circuit Model	Characteristics
2-Coil			<ul style="list-style-type: none"> Original type Short-range transmission
4-Coil (Conventional)			Comparing with 2-Coil: <ul style="list-style-type: none"> Higher power transfer efficiency Mid-range transmission
4-Coil (Asymmetric)			Comparing with the conventional 4-coil: <ul style="list-style-type: none"> Much higher coupling coefficient High power transfer efficiency with long transmit distance
3-Coil			Comparing with conventional 4-Coil: <ul style="list-style-type: none"> Higher power delivered to Load

Fig. 3: Comparison of two-coil, four-coil, and three-coil

from an AC source to an output loading resistance R . The electrical parameters can be calculated as below [18]:

$$C_p = \frac{1}{\omega L_p}; C_s = \frac{1}{\omega L_s} \quad (7)$$

$$L = \mu_0 N^2 \ln\left(\frac{8R}{a} - 2\right) \quad (8)$$

$$M = \frac{\pi \mu_0 r_1^2 r_2^2 N_1 N_2}{2d^3} \quad (9)$$

where μ_0 is the vacuum magnetic permeability. r_1 and r_2 are the radius of the transmitter coil and receiver coil, respectively. N_1 and N_2 are the turns of the transmitter coil and receiver coil, respectively. a is the wire diameter and d is the distance between transmitter coil and receiver coil.

2.3.2 Hybrid Compensation Circuit: Apart from the aforementioned four basic compensation topology circuits, there are several hybrid series-parallel compensation topology circuits found in the literature. (e.g., LCL, LCC, LC/S, LCCL.)

• **LCL compensation circuit:** [22, 25, 26] discuss the LCL compensation circuit applied to a WPT system. The advantages of LCL compensation topology circuits include a constant current source, high efficiency at light load (unity power factor), and harmonic filtering capabilities [27]. F. Lu *et al.* [23] give a comparisons of the three topologies of LCL compensation circuits (LCL-S, LCL-P, LCL-LCL), especially on their load characteristics comprehensively and systematically, as shown in Fig. 5. They point out that the primary inductance has an influence on the load characteristics when the LCL topology is utilized in the primary side.

In Fig. 5 LCL-S Compensation Circuit, L_1, L_2, R_1, R_2 are self-inductances and resistances of the transmitting and receiving coils, respectively. C_1, C_2 are compensation capacitors. R_L is the

equivalent load resistance. $L_{1'}$ is the series compensation inductor. The parameters of LCL-S network are generally determined by the following equation [28]:

$$\omega = \frac{1}{\sqrt{L_2 C_2}} \quad (10)$$

The receiving side resistance Z_s is:

$$Z_s = j\omega L_2 + \frac{1}{j\omega C_2 + \frac{1}{R_L}} \quad (11)$$

The equivalent impedance at the transmitting coil Z_r can be calculated as follows:

$$Z_r = j\omega L_{1'} + \frac{1}{j\omega C_1 + \frac{1}{j\omega L_1 + \frac{\omega^2 M^2}{R_L}}} \quad (12)$$

The parameters of LCL-P network are generally determined by equation as follows [29]:

$$\omega = \frac{1}{\sqrt{L_2 C_2}} \quad (13)$$

The total impedance of system Z_T is:

$$Z_T = j\omega L_{1'} + \frac{1}{j\omega C_1 + \frac{1}{j\omega L_1 + R_1 + \frac{\omega^2 M^2}{j\omega L_2 + \frac{1}{j\omega C_2 + \frac{1}{R_L}}}}} \quad (14)$$

Schematic	Primary Capacitance	Primary Quality Factor	Secondary Quality Factor
<p>(S-S) Series Compensated Primary and Secondary</p>	$C_p = \frac{1}{\omega_0^2 L_p}$	$Q_p = \frac{R L_p}{\omega_0 M^2}$	$Q_s = \frac{\omega_0 L_s}{R}$
<p>(S-P) Series Compensated Primary and Parallel Compensated Secondary</p>	$C_p = \frac{L_p}{\left(\frac{\omega_0^2 M^2}{R}\right)^2 + \omega_0^2 L_p^2}$	$Q_p = \frac{\omega_0 L_p L_s^2}{M^2 R}$	$Q_s = \frac{R}{\omega_0 L_s}$
<p>(P-P) Parallel Compensated Primary and Secondary</p>	$C_p = \frac{1}{\omega_0^2 \left(L_p - \frac{M^2}{L_s}\right)}$	$Q_p = \frac{R L_p}{\omega_0 M^2}$	$Q_s = \frac{\omega_0 L_s}{R}$
<p>(P-P) Parallel Compensated Primary and Secondary</p>	$C_p = \frac{\left(L_p - \frac{M^2}{L_s}\right)}{\left(\frac{M^2 R}{L_s^2}\right)^2 + \omega_0^2 \left(L_p - \frac{M^2}{L_s}\right)^2}$	$Q_p = \frac{\omega_0 L_p L_s^2}{M^2 R}$	$Q_s = \frac{R}{\omega_0 L_s}$

Fig. 4: The basic compensation circuit topologies of magnetic resonant coupling system [19–21]

Name	Schematic	Characteristics
LCL Compensation Circuit	<p>LCL-S LCL-P LCL-LCL</p>	<ul style="list-style-type: none"> LCL architecture has better light-load characteristics; LCL topology can achieve a peak end-to-end efficiency of 96%, and maintaining an overall higher efficiency even at its worst case; LCL topology has a perfectly constant current throughout the entire range of coupling; LCL topology can reduce the current stress of the bridge semiconductor by constraining the large reactive resonant currents of flow only in the resonant tank.
LCC Compensation Circuit	<p>LCC-LCC</p>	<ul style="list-style-type: none"> The characteristic of LCC topology greatly simplifies the control complexity in the primary side; LCC compensation at secondary side can achieve a unity power factor, which leads to high power efficiency; LCC topology has the characteristic of constant current both the input and output.
LCCL Compensation Circuit	<p>LCCL-LCCL</p>	<ul style="list-style-type: none"> LCCL topology can achieve a high efficiency with a high power level; LCCL topology can get constant output current at a specific frequency, which is not affected by the load and coupling coefficient.
LC/S Compensation Circuit	<p>LC-S</p>	<ul style="list-style-type: none"> Compared to double-sided LCC topology, LC/S topology increase the system efficiency, reduce power lost due to the reduction of compensation inductor; LC/S topology obviously reduce the difficulty of debugging the circuit to obtain ZVS and optimum performance.

Fig. 5: Hybrid compensation topology[22] [23][24]

C. Cai *et al.* [30] proposes the LCL compensation topology in the transmitter that can make the current constant in the transmitting

coil. Their method is still effective even if the reflected impedance of receiver changes due to the parking deviation and misalignment of EVs. LCL-S and LCL-LCL compensated wireless charging systems can output constant voltage and current, respectively, while both of them can realize the zero phase angle.

• **LCC compensation circuit:** The integrated LCC compensation topology for EV charging was presented by W. Li [31], which can reduce the size of the additional coil and make the system more compact with extremely high efficiency. S. Zhou *et al* [24] presented a multi-paralleled LCC compensation topology for dynamic EVs wireless charging, which can minimize the EMI and reduce the power loss of the system. A double-sided LCC compensation circuit topology was proposed by T. Kan, N. Rasekh and other researchers [32–36]. Fig. 5 shows a wireless charging system using the double-sided LCC compensation circuit topology. At the transmitting side, L_{f1} , C_{f1} , C_1 , and L_1 form the primary resonant part, which is tuned to have a resonant frequency equivalent to the switching frequency of the full-bridge inverter. At the receiving side, L_{f2} , C_{f2} , C_2 , and L_2 make up the secondary resonant part. Both the primary resonant part and the secondary resonant part have the same resonant frequency. To avoid energy exchange between the compensation inductors, the range of the vertical gap should be 140 mm–200 mm. The nominal gap is set to 150 mm accordingly.

The input impedance Z_{in} and secondary impedance Z_{sec} in double-sided LCC can be simplified as follows [32]:

$$Z_{in} = \frac{\omega^2 L_{f1}^2 L_{f2}^2}{M^2 R_{eq}} \quad (15)$$

$$Z_{sec} = \frac{\omega^2 L_{f2}^2}{R_{eq}} \quad (16)$$

$$R_{eq} = \frac{8}{\pi^2} R_L \quad (17)$$

In a double-sided LCC compensation network, $L_{f1}/(L_{f2})$ resonates with $C_{f1}/(C_{f2})$ while $L_2/(L_1)$ and $C_2/(C_1)$ are combined to resonate with $C_{f2}/(C_{f1})$. The resonant frequency ω can be calculated as follows:

$$\omega L_{f2} - \frac{1}{\omega C_{f2}} = 0; \omega L_1 - \frac{1}{\omega C_1} - \frac{1}{\omega C_{f1}} = 0 \quad (18)$$

$$\omega L_{f1} - \frac{1}{\omega C_{f1}} = 0; \omega L_2 - \frac{1}{\omega C_2} - \frac{1}{\omega C_{f2}} = 0 \quad (19)$$

The advantage of this topology is that it performs as a current source to both the input and output, and it can maintain relatively high efficiency at both light and heavy load conditions [35]. However, due to the high order system and the resonant mechanism, the operation of LCC compensation is very complex [32]. W. Li *et al* [36] presented a detailed comparison between the double-sided LCC and SS compensation topologies for EV wireless charging. The analysis proves that the double-sided LCC compensation topology is less sensitive to the variations of self-inductance caused by the change in the relative position of the primary and secondary coils. Generally, the double-sided LCC compensation topology outperforms the SS compensation topology in terms of efficiency and stability, other than the case when SS compensation topology is at higher mutual inductance value.

• **LC/S compensation circuit:** LC/S compensation topology was recently proposed by Y. Wang *et al*. [37]. The proposed LC/S compensation topology is shown in Fig. 5. L_P and L_S are the self-inductances of the transmitting and receiving coils, respectively. L_1 and C_1 are series compensation inductor and parallel compensation

capacitor in the primary, respectively. C_2 is a secondary series compensation capacitor. The circuit structure of an LCL-S compensation topology is completely identical to that of an LC/S compensation topology, but the tuning methods for compensation parameters are totally different. The LC/S possesses three degrees of design freedom (L_1 , L_P and L_S). U and M are not deemed as degrees of design freedom since they are generally unchanged. LCL-S only has two degrees of design freedom because L_1' must equal to L_1 . In addition, LC/S provides a strong capability of high-order harmonic suppression and better load independent voltage output than LCL-S topology [38]. LC/S compensation has all the major advantages of the double-sided LCC compensation topology. It comprises only three compensation elements, achieves higher power density while reduces system size as well as cost. As the maximum output power of LC/S compensated system can be easily changed by altering the value of L_1 and C_1 , in theory, the output power can reach infinity with the original input voltage and the operating frequency set to a calculated value. Additionally, compared to double-sided LCC compensation topology, the system efficiency of LC/S compensation topology is about 2.5% higher.

• **LCCL compensation circuit:** A. Ong *et al.* and J. Byeon *et al.* [39, 40] propose a compensation topology circuit where a parallel resonant tank is added to the series compensation, named as the LCCL compensation topology circuit, as shown in Fig. 5. Comparing with the series compensation circuit, the LCCL circuit produces high maximum transfer power. In addition, LCCL circuit produces high efficiencies with high transfer power levels with high coupling coefficients. S. Yang *et al* [41] presented a double-sided LCCL topology for wireless power transfer technology. In this system, a constant output current in the transmitting coil at a calculated frequency can be achieved, forming a stable alternating magnetic field that is not affected by the load and the coupling coefficient.

2.3.3 Topology of MRC WPT System: Fig.6 is the topology of the MRC WPT system. Q_1 - Q_4 are four power MOSFETs in the primary side, D_1 - D_4 are the secondary side rectifier diodes. The DC input is transformed into high-frequency AC power by a full bridge inverter. The high-frequency AC power generated in the primary resonant part is transmitted wirelessly through the main coupling between the two main coils. Finally, the AC power is converted back to DC by the rectifier where, after further filtering by the CL-filter, the resultant output is suitable to charge the battery packs.

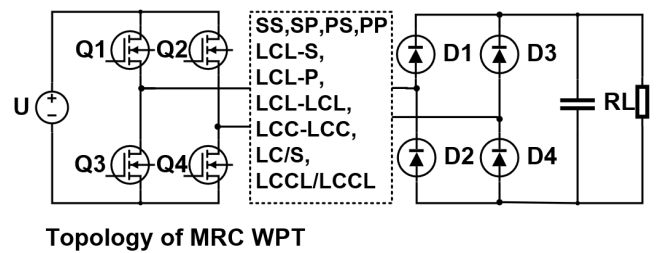


Fig. 6: Topology of MRC WPT System

2.4 International Charging Standards

The historically slow development of wireless charging techniques has held back the introduction of practical applications until recently, where major manufacturers have started to integrate it into electronic products. The biggest hurdle it currently faces is that there are several standard versions of the technology, making it difficult to offer chargers compatible across different devices. The following sections describe several of the main standards (the Qi, Alliance for Wireless Power (A4WP), SAE, and IEC standards).

2.4.1 Qi Standard: The Qi standard has been created by the Wireless Power Consortium and it is applicable for electrical power transfer over distances of up to 40 millimeters. Qi, pronounced as "Chee", is derived from an Asian word with its original meaning of "the vital energy", and has been used to indicate the intangible flow of power in the wireless charging process. The Qi wireless charging standard is mostly used in inductive wireless charging applications. A Qi wireless charger consists of two fundamental elements:

- **Base Stations:** The device that provides inductive power for wireless transmission. It contains a power transmitter whose major element is the transmitting coil. In practical cases the Qi charger is normally designed with a flat surface, namely the Interface Surface, thus the mobile device(s) can be placed on its top during charging procedure.
- **Mobile Devices:** The Qi mobile devices are those which consume the wirelessly transmitted power, whose internal batteries are to be charged by the base stations.

In addition, the Qi standard is integrated with a limited data transmission system between the base station and the mobile devices, such that the output of the base station can be adjusted based on the needs of the mobile device, and eventually terminate the power transmission once it is fully charged [42].

According to the range of power delivery ability, Qi wireless chargers can be classified as low power or medium power. The low power category covers chargers that can deliver power up to 5 watts. This can cover most devices, such as mobile phones, music players, and Bluetooth earpieces. While chargers in the medium power category can deliver power up to 120 watts. The frequency used for Qi chargers ranges from 110 to 205 kHz for the low power and 80-300 kHz for the medium power Qi chargers.

The position of the mobile device and base station is important because it is necessary to ensure the coupling between the transmit and receiver coil is as high as possible, thus the system can reach high efficiency. There are two types of positions:

- **Guided positioning:** This form of placement on a Qi charger involves the use of means to guide the user to place the mobile devices in the correct place on the Qi base station for charging. This is always implemented in the form of a single transmitter and a single receiver.
- **Placement anywhere:** The second form of Qi charger placement does not require the user to accurately place the mobile device on a particular area of the charging surface. Instead a wider area is usable. This can be achieved by using more than one transmitter coil.

As a matured standard the Qi certification has been adapted by a number of recently launched products, *e.g.* iPhone 8, iPhone 8 plus and iPhone X. Besides, There are thousands of Qi wireless charging spots in public spaces such as hotels, restaurants, coffee shops, bars, and transports [43].

2.4.2 A4WP Standard: The Alliance for Wireless Power (A4WP) is an independent industry body that was set up to develop and maintain the standards for a form of wireless power that allowed additional spatial freedom over the standards that already existed. A4WP uses a large area for the magnetic field, and this enables the device positioning requirements to be less critical, and it also allows a single power transmitter to charge multiple devices at any one time. Meanwhile, A4WP enables the possibility of Z-axis charging placement allowing the device to be detached from the charger [44].

There are several differences between the A4WP standards and other wireless charging standards. The features are discussed below:

- **Frequency:** An internationally available high frequency of 6.78 MHz is adopted to avoid inductive heating issues, which are commonly seen with tightly-coupled inductive systems under much lower frequencies.
- **Control and management protocol:** The frequency used for control and management is within the 2.4 GHz ISM (Industrial Scientific

and Medical) band. It is internationally available and is ideal for applications like smartphones and other electronic items.

There are two main elements in A4WP wireless chargers:

- **Power Transmitter Unit (PTU):** This is the unit that transmits the power to the unit requiring charging. The PTU contains two main parts, one comprises the areas used for the power transfer, and another is associated with the signalling.
- **Power Receiving Unit (PRU):** There are several classes of PRU dependent upon the application envisaged. Power enters the receiver via the resonator and it is rectified to provide a DC voltage. The rectifier needs to be able to provide efficient rectification at 6 MHz frequency. Once rectified, the power is converted to the required voltage using a DC-DC switch mode converter. Both the rectifier and the DC-DC converter can be controlled over the 2.4 GHz link to the charger to enable both charger and A4WP receiving unit to communicate to maintain power transfer at its highest efficiency.

2.4.3 SAE Standard: On May 17, 2016, SAE international approved TIR J2954 standard for PH/EV wireless charging. SAE International is a global association committed to being the ultimate knowledge source for the engineering profession. The key approaches of J2954 are determining minimum performance criteria for charging (efficiency) through team consensus with input from industry studies, otherwise, it can develop a common interface for vehicle side charging to assist in interoperability of wireless charging.

SAE TIR J2954 establishes a common frequency band using 85 kHz (81.39 - 90 kHz) for all light-duty vehicle systems. In addition, four PH/EV classes of WPT levels are given: 3.7kW (WPT 1), 7.7kW (WPT 2), 11 kW (WPT 3) and 22 kW (WPT 4). Future revisions may include even higher power levels [45]:

One key feature of TIR J2954 standard is the positioning. It includes XYZ tolerance, Rotation, Tilt, and Gap variation between pads, shown as Fig. 7. At the same time, the positioning methods are proposed as below, and communication is a key component of each method [46].

- **Triangulated RFID Positioning**
- **Magnetic Coupling Positioning**
- **Combination Positioning**

Currently, there are many wireless suppliers and companies involved in wireless charging using J2954, like Qualcomm, WiTricity and Evatran, *etc.*

2.4.4 IEC Standard: The International Electrotechnical Commission (IEC) has published IEC 62827-1; 2016, standard for wireless power transfer. IEC 61980-1:2015, the first Standard published in the series, covers general requirements for EV WPT systems including general background and definitions for example: efficiency, electrical safety, Electromagnetic Compatibility (EMC), protection from electromagnetic field (EMF) and so on. IEC 61980-2, part 2 of the series to be published later, will cover specific requirements for communication between electric road vehicles and WPT systems including general background and definitions. As for the third part in the series, IEC 61980-3, also scheduled to be published later, will cover specific requirements for EV magnetic field wireless power transfer (MF-WPT) systems [47].

IEC 62827-1:2016 specifies common components of management for multiple sources and devices in a wireless power transfer system, and justifies various functions for WPT. This part of IEC 62827 defines the reference models for possible configurations of a WPT system. The models are specified in additional parts in more detail. This standard is applied to WPT systems for audio, video, and multimedia equipment [48].

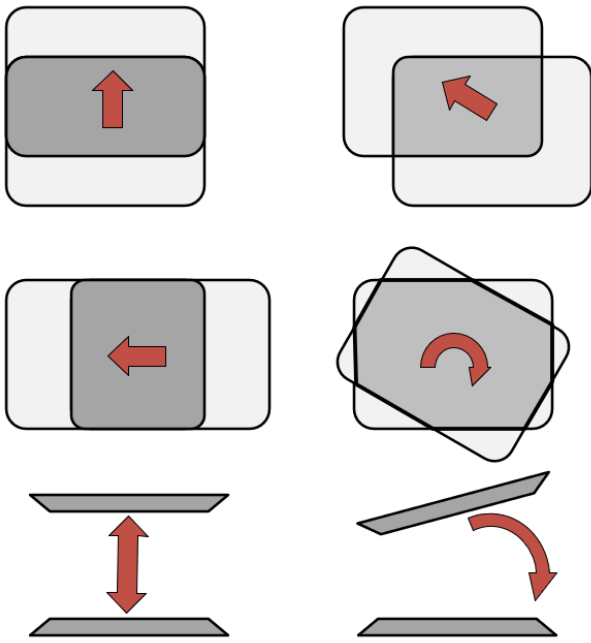


Fig. 7: The positioning in SAE Standard [46]

3 Wireless Electric Vehicle Charging

Renewable energy generation and Electric Vehicle (EV) technology has advanced in recent decades due to the pressing concerns about climate change, air pollution and energy security [49]. There were only 1.26 million battery EVs (BEVs) and plug-in hybrid EVs (PHEVs) by the end of 2015 (accounting for around 8% of global vehicle threshold) even though that almost doubled the number of 2014. Global sales of new EVs passed a million units in 2017, according to McKinsey's Electric Vehicle Index [50]. Under the current growth trajectory, EV producers could almost quadruple that achievement by 2020, moving to 4.5 million units, that is 5% of the overall global light-vehicle market. Nowadays, car companies have been developing various EVs such as pure BEVs, hybrid EVs, PHEVs, and roadway powered EVs. The hybrid EVs are more popular in worldwide markets among all EVs. Fig.8 shows a comparison of pure EVs in current market with battery type, range and charging time in wired charging case and wireless charging case, respectively.

However, at the current stage, it is unattainable to develop an electricity storage module (battery) that meets all the requirements for EVs, including high energy/power density, low initial cost, long cycle time, high safety level and stability. Until now, most EVs use plug-in charging. There are several weaknesses of plug-in charging, e.g., people may forget to plug-in and thus find themselves unexpectedly running out of energy; The charging cables on the floor can present trip hazards; the degradation of cables over time could prove dangerous to the user [51].

As far back as 2012, automakers have said they plan to include wireless charging technology on future EVs. Nowadays, wireless EV charging is already here, wireless charge pads and accompanying adapters for select plug-in models have been available at a price point within the reach of most plug-in buyer for several years. In 2014, Plugless Power began offering these kits for Chevy Volt, Nissan LEAF, and Cadillac ELR. In the years since, Plugless Power has expanded its lineup to service the BMW i3, Mercedes S550e, and Tesla Model S. The two biggest concerns with wireless chargers so far have been their speed and efficiency. Multiple wireless charging companies have demonstrated charging speeds of 20 kW or higher in tests. Wireless charge prototypes designed for trucks and public buses can even reach up to 250 kW. General Motors is currently working with WiTricity to develop a wireless charge system at 7.7

kW and 11 kW [52]. A comparison of these charging systems is shown in Fig. 9.

Presently, some automotive manufacturers together with governmental transport departments are actively investing in the development of dynamic wireless charging for EVs. Nissan achieved 90% efficiency for their low-power (1 kW) dynamic wireless charging system at low speed in 2013 [53]. Volvo, in collaboration with the Swedish Transport Administration, has been working on a dynamic wireless charging system for electric buses since 2015 [54]. Qualcomm developed and tested one of the worlds first dynamic wireless EV charging test tracks. The system is capable of charging an EV dynamically at up to 20 kW at highway speeds (100 km/h). In the UK, after the feasibility study of "Powering EVs on England's major roads" in 2015, Highways England set up an eighteen-month off-road trial to help meet their ultimate objective of promoting the deployment of EVs in the UK by installing wireless charging systems beneath roads. The UK government has earmarked £ 40 million for research programmes into wireless dynamic EVs charging, so that EVs could soon be able to charge their batteries wirelessly in public [55].

With the emerging concept of the smart grid, EVs play a new role: energy exchange with the power grid. These EVs are capable of not only drawing the energy from the power grid, but also delivering the energy back to the grid via the bidirectional charger [56]. Based on the charging/discharging capability of EVs and the energy-efficient requirement of the power grid, the vehicle-to-home (V2H), and vehicle-to-grid (V2G) concepts have become more and more attractive in recent years. In January 2019, Honda presented a wireless V2G system which was developed with WiTricity [57]. It is anticipated that wireless V2G, V2H and vehicle-to-vehicle (V2V) concepts will probably become a reality in the very near future.

In this section, we will discuss the design of static wireless and dynamic wireless EVs charging systems.

3.1 Static Wireless EV Charging

The block diagram of a wireless EV charging system is shown in Fig. 10. There are several constraints to the design of static wireless EV charging system, as below:

- Increase magnetic coupling as much as possible to obtain higher induced voltage;
- Increase power transfer efficiency (PTE) for given power capacity and cost;
- Make the model as compact as possible to fit a given space and weight;
- Manage changes in resonant frequency and coupling coefficient due to misalignment of pick-up position, and air-gap variation.

The main research issues of static wireless EV charging systems can be summarized as follows:

3.1.1 Power Transfer Efficiency (PTE): The major defects of the wireless EVs charging technology are lower PTE and low pick-up power [58]. Recent research has focused on the methods for improving PTE in wireless EVs charging systems. Theodoropoulos *et al.* proposed a load balancing control algorithm for wireless EVs charging to increase efficiency [59]. Some studies have investigated different types of primary power supply architectures for wireless EVs charging for maximum efficiency [60, 61]. T.Kan *et al.* proposed a wireless charging system using a double side LCC compensation topology; a compensated coil into the main coil structure to get high efficiency [62]. C. Cai *et al.* proposed a dynamic LCL-S/LCL switch topology in wireless EVs charging system, which can achieve a constant current in transmitting coil and constant voltage output [63]. Some researchers have focused on new materials, such as Y.D.Chung *et al.*, who proposed a high-temperature superconducting (HTS) resonant coil to improve PTE [64]. The coil structure design and location will also affect PTE in wireless EVs charging [65–67].

Model	Battery	Wallbox Charge Time	Fast Charge Time	Wireless Charge Time
Peugeot e-208	50kWh, range:211 miles	5 hrs (11 kW)	30 mins to 80% (100kW)	
Mercedes EQC	80kWh, range:280 miles	12 hrs (7.4 kW)	40 mins to 80% (100kW)	
Audi e-tron	95kWh, range:248 miles	9 hrs (11 kW)	30 mins to 80% (150kW)	
BMW i3	42.2kWh, range: 160 miles	4 hrs (11 kW)	42 mins to 80% (50kW)	Charging input voltage:240V; 30/50 Amp Circuit; 11 kW charger: 4-5 hours
Citroen C-Zero	14.5kWh, range:93 miles	7 hrs (3.7 kW)	30 mins to 80% (50kW)	
Hyundai Ioniq Electric	28 kWh, range: 174miles	4.5 hrs (7.4 kW)	25 mins to 80% (50kW)	
Jaguar I-Pace	90kWh, range: 292 miles	13 hrs (7.4 kW)	45 mins to 80% (100kW)	
Kia e-Niro	64kWh, range: 282 miles	10 hrs (7.2 kW)	45 mins to 80% (60kW)	
Nissan Leaf	40kWh, range: 168 miles	7 hrs (6.6 kW)	40 mins to 80% (50kW)	Charging input voltage:240V; 30 Amp Circuit; 7.2 kW: 6 hrs
Tesla Model 3	75kWh, range: 338 miles	5 hrs (11 kW)	30 mins to 80% (120kW)	
Tesla Model S	100kWh, range: 393 miles	7 hrs (16.5 kW)	40 mins to 80% (120kW)	Charging input voltage: 240V; 50 Amp Circuit; 11 kW Charger: 20-25miles of range per hour parked.

Fig. 8: EV battery information and power transfer level comparison of charging methods

Features	Plugless Power	Qualcomm Halo	Witricity (DRIVE 11)
Technology	Inductive charging	Resonant magnetic inductive	Magnetic resonant coupling
Normal charging gap	4 in (10 cm)	No mind the gap (high energy transfer over a wide air gap)	Low: 10cm-15cm Med: 14cm-21cm High: 17cm-25cm
Standards	NEC 625 (NFPA 70), SAE J1772, UL 2231 and CSA 170.1	ISO, IEC and SAE	SAE TIR J2954, IEC and ISO
Power transfer rates	GEN 1 system: 3.3 kw-7.2 kw GEN 2 system: 7.2 kw	3.3 kw-6.6 kw	WPT1: 3.6 kw WPT2: 7.7 kw WPT3: 11 kw
Efficiency	3.3kw output with 10cm gap: 88.8%	>90%	Up to 94% grid to battery
Test	GEN 1 system: Chery Volt Nissan LEAF GEN 2 system: Tesla Model S BMW i3	3.3 kw and 6.6 kw: Delta E-4 7 kw: Rolls Royce Phantom 102EX 20 kw: Drayson B12/69	Delphi Automotive
Others	Get 20-25 miles of range per hour parked	Power transfer solutions have been developed to suit a broad range of vehicle types	Parking freedom: X-Y-Z

Fig. 9: Comparison of Plugless, Qualcomm Halo, and Witricity

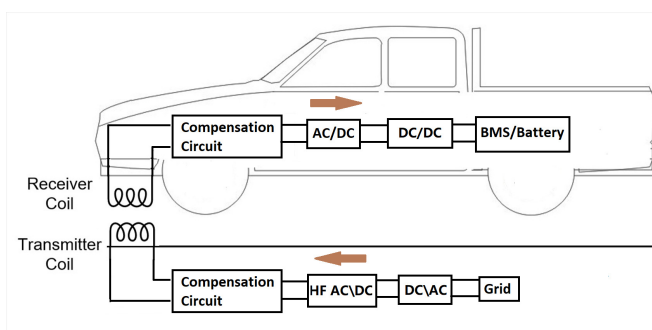


Fig. 10: The block diagram of the wireless EV charging system

The most immediate cause of the lower PTE is the low coupling coefficient induced by a loosely coupled transformer, *e.g.* the misalignment between transmitter and receiver coils. Meanwhile, the packaging constraints of most vehicles limit the size of TX and RX coils [68], thus constrain the implementation of WPT, since the existing WPT systems are bulky and highly sensitive to axial and angular coil misalignment [69–74]. Recent research explores mitigating techniques such as adaptive matching networks [75] and arrayed TX coil structures [76–78]. Y. Gao *et al.* propose an alignment sensing

system which is based on magnetic sensing that employs multiple auxiliary minor coils on the secondary side to position the charging pad [79]. L. Zhao *et al.* presents a hybrid wireless EVs charging system which uses a combination of the different resonant networks to fix the pad misalignment [80].

3.1.2 Coil Design: Optimizing the coil material can improve the system's PTE. A high Q planar-Litz coil has been proposed which can promote efficiency by up to 40% when the transfer distance is 0.5 cm [81]. The coil is designed by dividing the wide planar conductor lengthwise into multiple strands to reduce the high frequency conduction losses and to improve the Q-factor. T. Mizuno *et al.* proposes a magnet plated copper wire whose circumference is plated with a magnetic thin film which increases the inductance. Meanwhile, the resistance due to the proximity effect is decreased because eddy current loss is reduced [82].

The coil size is one important parameter in MRC WPT system design. A major design constraint for the coil is the space limitation [83], *e.g.* receiver coil size for biomedical implants should be small, while the transmitter coil size can be large. However, for EV charging or industrial applications, both the transmitter coil and the receiver coil can occupy large spaces. The ratio of the coil diameter and transmit distance (air-gap) can also affect the transmission efficiency. Assuming a constant Q-factor, if the air-gap (L) is smaller

than half of the coil diameter (R), i.e., $L/R < 0.5$, the transmission efficiency will exceed 80%. Furthermore, if $L/R < 0.25$, the transmission efficiency can reach 90% [84].

The coil geometry also has effects on transmission efficiency. Solenoidal coil, flat (or spiral) coil, square coil, and circular coil have different efficiency according to the literature [85–87]. The flat coil is widely used in magnetic resonant coupling WPT system. Z.Pantic gives some experimental comparisons between the solenoidal coil and spiral coil [88]. J.P.K Sampath *et al.* [83] and M.Q.Nguyen *et al.*[89] propose an experimental analysis of different types of flat (or spiral) coil design. The power transfer and transmission link efficiency of the spiral coil can be improved by tuning three geometric parameters which have an effect on the radiation patterns, namely inner radius, outer radius, and turn number. M.Q.Nguyen proposes a method to adjust the parameters and eventually optimise the design of the spiral antenna regarding both field intensity and circuit efficiency [89].

The Litz wire diameter and the number of turns are two parameters for coil design. Optimising the design of the coil can be performed by either tuning the Litz wire diameter or the number of turns. The Litz wire diameter should be selected by the current of the coil, and the number of turns should be designed by the mutual inductance or the required power output. The space between wires influences the coupling since the leakage flux tends to directly close from the wire space. The smaller wire space leads to a higher coupling coefficient [65]. Ferrite cores are widely used in wireless EV charging design to increase the PTE, however, it has a tradeoff between the weight and coupling coefficient. The shielding which is added to both the primary and secondary coils is an important design for the wireless EV charging system. The shielding in the primary coil is designed to block the magnetic flux from going down to the metal plate below the floor-board of the garage to cause eddy current loss. The shield is designed to cut off the magnetic flux in case it goes into the chassis of the vehicle, which may put the humans in danger as well as causing energy loss.

3.2 Dynamic Wireless EV Charging

Even though dynamic wireless charging prototypes for EV are continuously proposed and improved upon for higher efficiency and lower costs, they are rarely commercialized and the existing commercial operations are limited to electric buses and trams, operating at low speeds in urban areas [90, 91]. One of the potential reasons for this is the difficulty in precisely predicting and fast responding to the charging demands of an EV, particularly a private EV, for dynamic wireless charging systems. Unlike the 'controllable' public electric buses that have fixed routes and almost fixed speeds due to the arranged schedules, the driving behavior of private EVs is unpredictable as it is influenced by many factors such as personal habits, traffic conditions, climate, and contingencies. A high fluctuation of demand is expected due to the sparse monitoring infrastructures and higher driving speed.

Another reason may lie in the stricter operation requirements of dynamic wireless charging for EVs. Unlike the plug-in charging and static wireless charging which normally lasts for hours at low power rating, the dynamic charging period varies from a few seconds to minutes, depending on factors including the driving speed, charging lane configuration and charging schedule [92]. Thus, dynamic wireless charging requires much higher charging power and faster balancing response from the charging system and power supply ends [92–94]. Additionally, in order to ensure the efficiency and extend the charging time, the existing dynamic wireless EV charging prototypes are limited to fixed slow speeds. Subsequently, more energy will be consumed. This may pose a great strain on the electrical grid if more EVs are purchased and more dynamic wireless EV charging systems are installed and connected to it, particularly during peak demand time. Situations may even worsen if fossil fuels are still used as the dominating energy sources resulting in increased carbon emissions.

Most roadway WPT systems adopt an elongated loop of wire as the primary line of the power supply, such as the roadway-powered

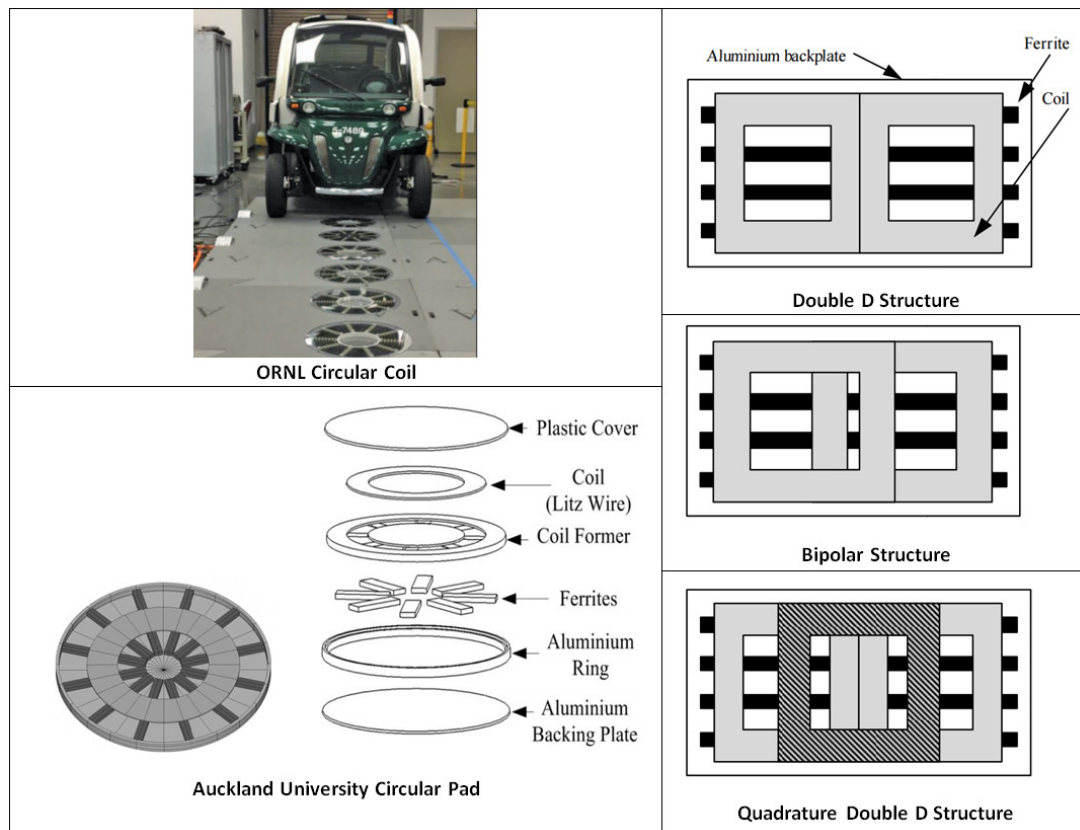


Fig. 11: Pad form in dynamic wireless EV charging system

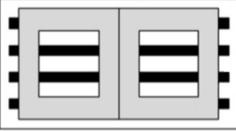
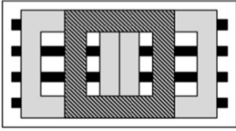
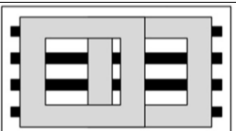
Type	Feature
 <p>DD Pad</p>	<ul style="list-style-type: none"> • Single sided flux generation • Perform better and be interoperable with different secondary topologies • Commonly used in the primary • Ferrite bars easy to be saturation at high power rate • No reverse flux to eliminate the unwanted rear flux
 <p>DDQ Pad</p>	<ul style="list-style-type: none"> • As a secondary, providing z charge zone three times than DDP • Perform better with different secondary topologies • Commonly used in the secondary • Variable excitation modes • Inferior material usage efficiency • Versatile in central coil design to fit the airgap
 <p>BDD Pad</p>	<ul style="list-style-type: none"> • Mutually decoupled partially overlapped coil structure • Almost the same performance of DDQP used as a secondary • Using less copper than DDQP • Perform better with different secondary topologies • Commonly used in the secondary • Almost identical power with DDQ for given size

Fig. 12: The Feature of DD pad, DDQ Pad, and BDD Pad [56]

EVs (RPEVs) and online EVs (OLEV) system, while other systems choose circular-type coils. Despite its technological advances comparing with static wireless EV charging, dynamic wireless EV charging is struggling to perform robustly under large variations of lateral misalignment, air-gaps, ambient temperature and humidity, mechanical shocks and road surface conditions. In addition, its cost will have to be further reduced so as to make it commercially viable.

There are several design issues with dynamic wireless EV charging as follows:

- **Segmented Power Supply Rail:** Segmented power supply rails are the optimal choice for the dynamic wireless EV charging rails. Each segment should be turned ON and OFF independently, so it requires a large number of compensation components and power electronic converters. In addition, the length of the segmented rail is an important design issue because it would be too expensive if the number of inverters or switch boxes are increased due to the very short lengths. On the other hand, the PTE will decrease if the resistance is increased due to very long lengths.
- **Power pulsation phenomenon:** One big challenge in dynamic wireless EV charging system is the output power pulsation. If the dynamic wireless EVs charging system is of the segmented supply rail type, the distance between adjacent segments and car length should be considered in a dynamic wireless EV charging scheme. The distance between the adjacent transmitters is large enough that the power pulsation is unavoidable, but the self-couplings can be neglected. If the separated distance keeps decreasing, the power pulsation is further reduced, and the self-couplings between the transmitters have to be considered in the compensation circuit design. F. Lu *et al.* proposed an analysis of rail design in dynamic wireless EVs charging systems which can reduce power pulsations during the charging process. The system used multiple rectangular unipolar coils at the primary side and another unipolar coil operates as a receiver at the secondary side [23]. S.Cui proposed a multiphase receiver in the dynamic wireless EVs charging system to reduce the

output power fluctuation [95]. Y. Wang *et al.* presented the DDQ type of the receiver coil and double-side LCC topology can optimize the system design to solve the output power pulsation problem [96].

- **Coupling coefficient Variation:** Due to the inevitable lateral misalignment and air-gap variation during charging, this can affect the magnetic coupling between a power supply rail and pick-up charger, and the coupling coefficient of dynamic wireless EV charging system may fluctuate greatly [17]. In addition, when the number and type of cars on the power supply rail changes, the coupling coefficient changes, which further increases the need for smart coil design or inverter design to cope with this fluctuation.
- **Roadway Construction:** For static wireless EV charging, the charger can be designed as a pad, settled on the garage floor or under the car park without any environmental impact. However, dynamic wireless EV charging should adapt to various roadway conditions. Most of these conditions are unpredictable and uncontrollable, *e.g.*, scattered debris, dirt, snow, *etc.*. Therefore, many variables must be considered when designing the system.

The pad form design and power supply rail design are fundamental issues of dynamic wireless EV charging system design:

3.2.1 Pad Form Design: In wireless EV charging systems, the coupler is usually designed in a pad form. Oakridge National Laboratory (ORNL) started their investigation into inductive dynamic wireless EV charging in 2011. They are the first group that discovered that the circular coil topology can achieve smaller lateral tolerance while capacitor regulation at both supply and receiving sides can effectively smooth power pulsation [98]. In the 1990s, Auckland University presented a novel circular pad structure (as shown in Fig. 11). These power pads overcame several physical limitations of common couplers by using multiple smaller bars. (*e.g.*, a coil former with further protection provided by the aluminium and plastic case.) The circular power pads were relatively thinner compared to standard core topologies, and they were lighter than conventional circular coupler designs that used solid ferrite discs. Coupling could be improved in this design compared with a single ferrite bar. Abba Hariri *et al.* [99] presents a circular pad design that takes the effect of the magnetic core and the conductive shielding layers. Moreover, they proposed the Pareto optimality algorithm to maximize the coupling factor and the quality factor for the coils of the dynamic wireless EVs charging system. The circular coil is a popular choice in dynamic wireless EVs charging design, however, it has restrictions on air-gap length and high output power [100]. The circular-type coils were inadequate for high-power road-power EVs because of their low-power transfer capability and small lateral tolerance [101].

In 2011, M. Budhia *et al.* [102] proposed a single-sided polarized pad called the "Double D", as shown in Fig. 11. It was formed using two coils which were wound to form a north and south pole internally according to the layout of the coils and must be driven in series by a single phase inverter. The ferrite was placed behind the coils which had been arranged into four discrete rows with an air-gap between each row. The DD pad has significant better coupling than a circular pad. Other than the novel primary polarized pad design, a new generic magnetic receiver was proposed called the "Quadrature Double D", shown in Fig. 11. Comprised of the Double D structure, a third coil was added in the center of the pick-up. From the experimental results, power transfer in this design significantly increased and the structure could achieve a higher tolerance to misalignment.

After the double D structure, a Bipolar DD structure was proposed which consisted primarily of two coils of wire. The coils were partially overlapped and mostly coplanar unless one of them must be lifted slightly to pass over the other, shown in Fig. 11, the amount of overlap, in this case, was chosen so that the mutual inductance between the two coils was ideally zero. The ferrite was placed behind the coils, as with the double D [103]. The Bipolar DD coil configuration produces a lower maximum power transfer when the two coils are operated with their currents offset in phase by 90° than a similarly sized configuration with the currents operated in-phase. However, the power transfer drops more slowly with offset, and can thus produce a system with higher tolerance to misalignment.

T. Nguyen *et al* carried out a feasibility study on bipolar DD pad. The rectangular bipolar DD coil had better misalignment tolerance than the circular type [104]. Paper [65] presented an analysis of the comparison of the double D (DD) coil and the unipolar coil. Moreover, the research focuses on the coil structure design to achieve the maximum coupling coefficient in the misalignment case and provides the optimized sizes of the unipolar and DD type loose coupled transformer for wireless EV chargers. The results showed that the coil sizes are designed to have the maximum coupling coefficient and efficiency. The achievable maximum efficiency is linear with the size of the secondary coil pad. Z. Zhang *et al* [105] present a comparative analysis of the various transmitter coils (circular shape, rectangle shape, and multi thread), as shown in Fig. 13 and the receiver is a DDQ coil. The results show that the rectangle-shaped and multi-thread primary coil can offer higher charging power compared with the circular-shaped primary coil. Furthermore, compared with the rectangle-shaped coil, the multi-thread primary coil has the advantage of greater misalignment tolerance and heating dissipation. There are some other topologies of DD coil, like crossed DD coil [106], and the unequal DD coil [107]. A comparison of the DD pad, DDQ pad, and BDD pad is shown in Fig. 12.

3.2.2 Power Supply Rail Design: The ground-side track power supply is a key part of the dynamic wireless EVs charging system. The single power supply rail design is the pioneering structure of dynamic wireless EV charging rail, as shown in Fig. 14a. The single rail track is easy to supply power to and had a simple structure [108], however it causes extra power losses and electromagnetic field radiation if there is no EV charging. The segmented rail is the mainstream design nowadays [109]. This configuration greatly reduces the required number of power supplies for charging multiple EVs and solves the single rail's problem. Several structures of the segmented tracks were presented as follows:

Fig. 14b shows a simple system with the power supply running along the roadway and transfers power to individual sections through direct connections. The advantages of this segmented rail are decreased power loss due to the option that different segments can be turned on at different time periods. Moreover, this design has

high reliability, when one of the segments breakdowns, other segments can still function normally. The drawbacks of this design are the high number of converters required can add increase the complexity of control and increase the maintenance and construction costs.

Fig. 14c is similar to Fig. 14b in that direct connection is used between the power supply and all charging sections. The difference is that only one power converter is used in the central power unit [110]. This design reduces the number of power converter units and is, therefore, easier to maintain. The disadvantages of the design are a high loss in the cable connecting the power supply to the segmented rails; when the power supply breaks down, all of the segmented rails will stop functioning, thus lowering the system's reliability.

Fig. 14d shows a double coupled configuration rail that transfers power from the power supply through a magnetic coupler to each charging section rather than via direct connection. A simple switch (such as a bidirectional ac switch) is then used to control the turn ON and OFF of each individual section [111, 112]. The drawback of this design is a high requirement of capacitors because they need to carry full track current at the frequency of operation. Qi Deng [113] presents a segmental track coil without a position sensor. The method decides the power switching time through detecting the changing of the phase angle, and every coil is energized by an ac power circuit (from an inverter) through a relay.

3.3 Research Trends of Dynamic EVs Charging

3.3.1 Korea Railroad Research Team: One leading research group is the Korea Advanced Institute of Science and Technology whose On-line Electric Vehicle (OLEV) is market ready. Launched in 2009, the OLEV has undergone six generations of development applying MRC WPT technology. This project solved several problems such as Low EMF characteristics, further reduction of the construction cost of time for OLEV with narrow-width power rail, large lateral tolerances, and segmentation of power rails.

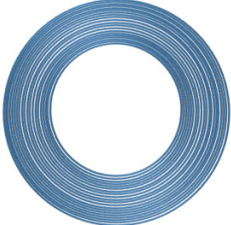
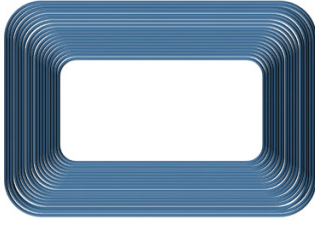
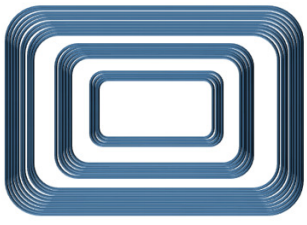
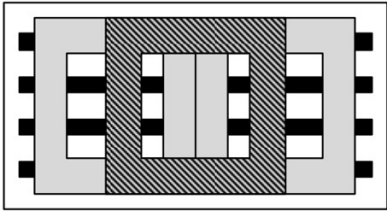
Parameters	Circular Shaped	Rectangle Shaped	Multi Thread
Type Primary	 Size: 600mm *600mm	 Size: 800mm *600mm	 Size: 800mm *600mm
Type Secondary	 DD-Quad (DD 400mm*600mm; Quad: 500mm*600mm)		
Air gap	200mm		
Power	7.84 kW	14.04kW	14.01kW
Cost Per/kW	1.998 £	1.334£	1.399£
Anomaly coefficient	43.8%	56.6%	51.5%

Fig. 13: Comparison between the circular-shaped, the rectangle-shaped and the multi-thread [97]

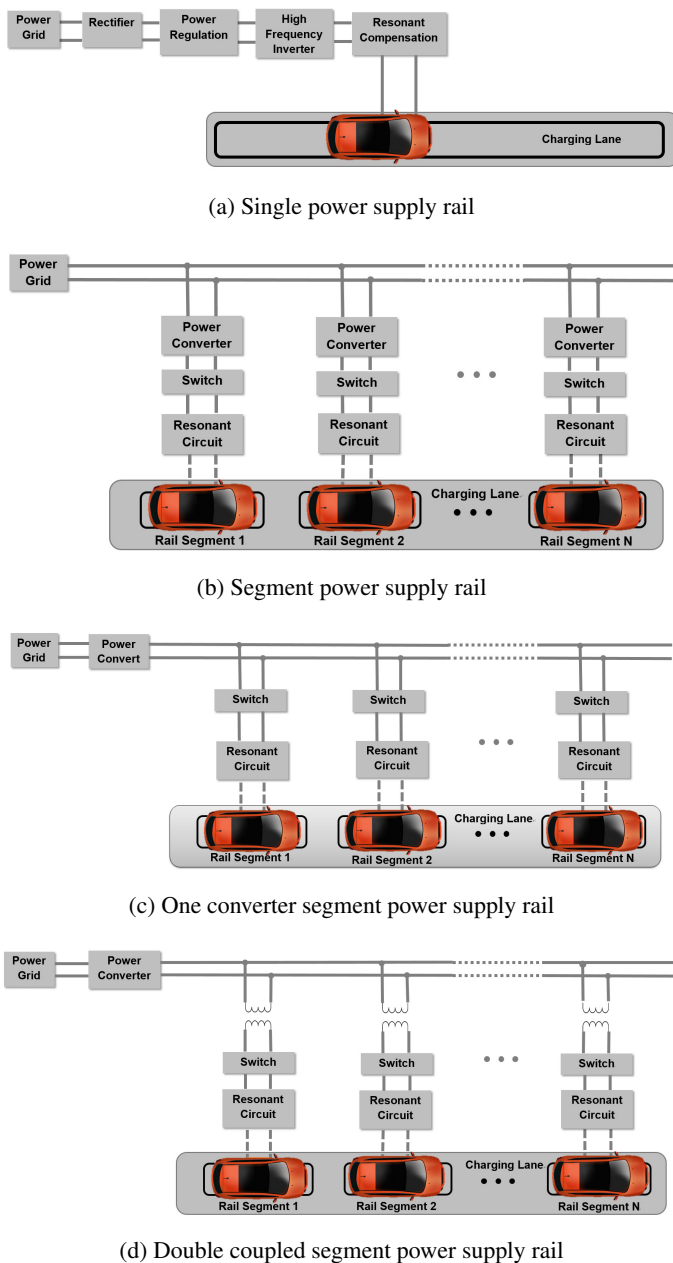


Fig. 14: Power supply rail structures

- The 1st generation of OLEV: The 1G OLEV golf bus was announced on 27 February 2009, and used an E-type core power supply rail. Fundamentally, its structure was similar to the E-type cored transformer. The primary core was an E-type segmented structure with a mechanical supporter, and the secondary pick-up was a conventional E-type structure. As a transformer, lateral misalignment of both cores severely degraded output power. This misalignment could happen frequently during driving if it was not for the mechanical lateral position control for pick-up with 3mm accuracy. Using these structures, an 80% system power efficiency was obtained with a 1cm air-gap. At the primary side, the nominal frequency was 20 kHz and the rated current was 100 A. At the secondary side, the rated load was 2 Ohm and 3kW per pick-up was obtained. The biggest weakness of the 1G OLEV is the limitation of the air-gap, but it successfully demonstrated the wireless power delivery to a running car [114].

- The 2nd generation of OLEV: The 2G OLEV bus was announced on 14 July 2009 and used an ultra slim U-type core power supply rail. In the 2G OLEV system, the nominal frequency of power supply was 20kHz and primary rated current was 200A. The rated load was 6kW per pick-up. The total output power of 52kW with 10

pick-ups and 72% power efficiency was accomplished with a 17cm air-gap. The distinction of the 2G OLEV was the direction of magnetic flux. The U-type core power supply rail structure was proposed with the direction of magnetic flux at center position being parallel to the ground, with each end position having significant fringe effects. The pole width of the primary core was much smaller than the length of the pick-up coil. So the effective pick-up width increased as the air-gap increased. Therefore the magnetic flux transferred from the primary coil to the pick-up coil was proportional to the root of the air-gap. In the 2G OLEV system, the proposed core structure made it possible to achieve about 50% power transfer from the primary coil to the pick-up coil with 20 cm misalignment. Comparison with the 1G OLEV, the air-gap increased from 1cm to 17cm, and without mechanical control apparatus. However, the primary rail length of the 2G OLEV increased to 140cm due to the return cables for reducing EMF. That meant the construction cost increased and out power was limited. To solve this problem, the 3rd generation of OLEV was proposed [114].

- The 3rd Generation of OLEV: The 3G OLEV sports utility vehicle was launched on 14 August 2009 and used an ultra slim W-type structure which did not need the return cables. The ultra slim W-type had a narrow primary core pole width and wide pick-up core length meaning it could transfer power with a large air-gap. The return path of the magnetic flux in the ultra slim W-type was doubled, therefore the transferred power from the primary core to the pick-up could be increased, however, the maximum allowable lateral misalignment was roughly a quarter of the length of the primary coil [114]. In the 3G OLEV with a fish bone like core structure, the amount of the core was reduced by 1/5 compared to the 2G OLEV, but the output power was improved to 17kW per pick-up. The measured power efficiency for the 3G OLEV SUV was 71% with a 17cm air-gap at the same nominal primary frequency and current as the 2G OLEV case.

- The 4th generation of OLEV: The 4G OLEV bus was announced in 2010 with a narrow rail width of 10 cm, a small pickup with a large lateral displacement at about 24 cm, and a large air-gap of 20 cm was proposed. The maximum output power of 35 kW and the maximum efficiency of 74% at 27 kW was achieved. The 4G OLEV proposed an I-type power supply rail, where the name "I-type" stems from the front shape of the power rail. In an I-type structure, each magnetic pole consists of ferrite cores and a turned cable, and the poles are connected to each other with a ferrite core. Due to this alternating magnetic polarity of adjacent poles, the EMF for pedestrians around the power supply rail could be drastically reduced and large lateral displacement could also be achieved by the wide pick-up [115, 116]. A significant improvement of 4G OLEV was lateral tolerance as well as a large air-gap, high power efficiency, lower construction cost, and time reduction. However, the construction cost and time of the power supply rail should be further reduced for better commercialization because the construction cost of the power supply rail was critical for deploying the dynamic EV charging and longer construction time resulted in more traffic jams and extra deployment costs.

- The 5th generation of OLEV: The 5G OLEV bus was announced in 2012. It proposed an ultra slim S-type power supply module with a 4cm width which could further reduce the construction time and cost for commercialization. The name "S-type" stems from the front shape of the power supply rail. Each magnetic pole consisted of ferrite core plates and power cables, and adjacent magnetic poles were connected by bottom core plates. The EMF on pedestrians in close proximity the power supply rail is significantly reduced due to the opposite magnetic polarity of adjacent poles. From this result, it was estimated that the S-type version has a lower EMF than the I-type version because the width of the S-type was narrower than that of I-type. The maximum efficiency of the 5G OLEV was 71% at 9.5kW and the maximum pick-up power was 22kW with an air-gap of 20cm. The S-type one led to a reduction in the construction cost and time for commercialization of dynamic EV charging and a further reduction for the EMF generated from a power supply rail for pedestrians. Moreover, it could lead to larger lateral tolerance of a charging system [117].

- The 6th generation of OLEV: The 6G OLEV proposed a universal wireless power transfer (U-WPT) system which could be applied to both road-powered EVs and general EVs. General EVs could not

only be charged in a conventional stationary charging station, but also could be charged when they were moving along a road by the power supply rails of the proposed U-WPT system installed underneath the road. This U-WPT system adopted a new coreless power supply rail to increase its operating frequency from 20kHz to 85kHz. The coreless type meant that no ferrite core plate was installed under the power supply cable. The power supply rail was an important part for a dynamic EV charging system design, and the shape of the proposed coreless power supply rail was basically the same as the U-type and W-type power supply rail [118]. For road-powered EVs, the power supply rail of an OLEV design was developed by KAIST, which showed good performance with a high efficiency rate of 83% and a long air-gap of 20 cm, and operated at the frequency of 85 kHz used by general EVs. The coreless power supply rail had several benefits compared to the with-core power supply rail, such as a lower cost, less insulation voltage stress, the absence of core loss, and less sensitivity to lateral misalignments for the same power rating [119].

3.3.2 Oak Ridge National Laboratory (ORNL) Research Team: The ORNL dynamic EV charging project started in 2011. ORNL team demonstrated dynamic EV charging in test drives of the Global Electric Motors (GEM) EV over an energised track consisting of six primary coils. Each coil was planar spiral wound with seven turns using cable guides interspersed with wedge-shaped ferrite flux guides. The ferrite plates were covered with a Kapton sheet for voltage isolation. The circular coil was designed for operation at 48kHz. J.M.Miller [98] presented one ORNL dynamic EV charging system, where the power level was controlled by the HF inverter rail voltage. The primary coils connected in pairs and in phase (*i.e.*, fountain field), each tuned to 22 kHz. The coil sequencing was

controlled by a vehicle passage using a trackside photocell interruption. In this dynamic charging system, the passive and active parallel lithium-capacitor (LiC) unit was used to smooth the grid-side power and Zlinx radio communications between the vehicle and grid-side controller. The Maxwell Technologies carbon ultracapacitors (UCs) pack was used in parallel with a demo vehicle battery pack.

One important aim of the ORNL dynamic wireless charging system was to demonstrate grid-side and in-vehicle power smoothing. Dynamic EV charging could cause power pulsations in the vehicle battery and the grid supply. These pulsations were due to the motion of the vehicle capture coil as it passed over a series of roadway embedded coils and the resultant pattern of alignment and straddling of their magnetic fields. The battery charging with a pulsating current could deteriorate the battery service life. In order to solve this problem, the local power storage of ORNL used two different high-power capacitor technologies: a pack of carbon UCs fabricated at ORNL and operating in passive parallel with the GEM EV battery pack and LiCs operating in active parallel with the grid-side power supply. Active parallel meant that a high-power, bidirectional controllable power flow, DC-DC converter interfaced the LiCs to the DC input of the WPT HF inverter. The experiment results showed that the vehicle charging current could be smoothed when using carbon UC and that the power pulsations were absorbed by the LiC as expected.

3.3.3 Auckland University Research Team: In 2014 the Auckland University research group proposed a new roadway for road-power EVs using a double-coupled system [120] which had an intermediary coupler circuit (ICC) with frequency changing capability between the power supply primary track and each ground transmitter pad/coils. The proposed double-coupled system used an elongated primary track to power multiple EVs while at the same

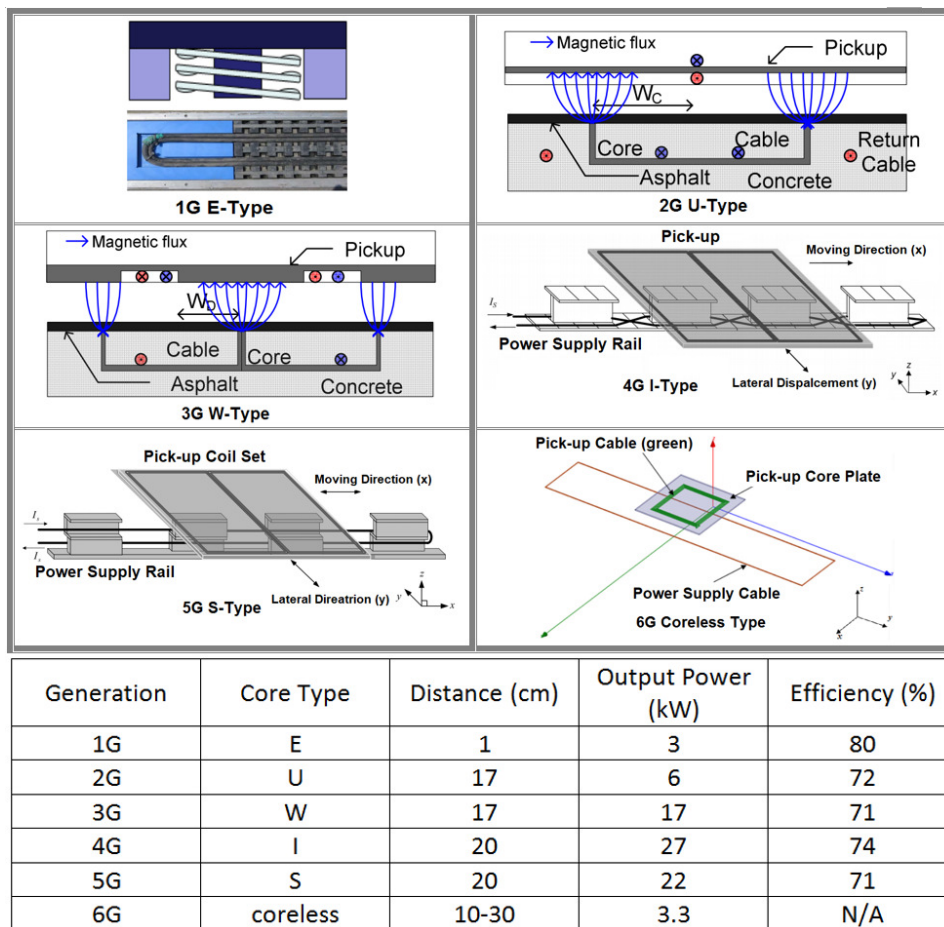


Fig. 15: KAIST wireless dynamic EV charging

time it allowed independent control of individual charging sections through the use of an additional circuit called an intermediary coupler circuit (ICC) that allowed frequency changing and synchronization without reflecting unwanted volt-ampere reactive (VARs) onto the backbone supply.

4 Conclusion

Wireless power transfer (WPT) technology is currently undergoing intense research in both academia and industry. Magnetic resonant coupling (MRC) WPT plays an important role in WPT technology. Compared with other WPT techniques, MRC WPT has higher power transfer efficiency with longer transmit distance. Meanwhile, there are several issues of MRC WPT, such as misalignment tolerance and load variation tolerance. High power transfer efficiency is a common goal for all WPT techniques. By improving the design of the coil and the circuit, the power transfer efficiency can be improved. One important application of MRC WPT technology is wireless EV charging. There are two primary implementations of wireless EV charging, namely static wireless EV charging and dynamic wireless EVs charging. Wireless EV charging technology can improve the user experience of EVs and offer greater flexibility. Dynamic wireless EVs charging can reduce the battery capacity requirement, extending the driving range of an EV. The future uptake of wireless EV charging faces several challenges including cost, standardisation, and health and safety.

5 References

- 1 Shen, F.Z.: 'Circuit analysis of wireless power transfer by "coupled magnetic resonance"', *IET Conference Proceedings*, 2009, pp. 602–605(3)
- 2 Lang, H.D., Ludwig, A., Sarris, C.D. 'Optimization and design sensitivity of siso and miso wireless power transfer systems'. In: 2015 IEEE International Symposium on Antennas and Propagation USNC/URSI National Radio Science Meeting. (, 2015, pp. 406–407
- 3 Bou.Balust, E., Hu, A.P., Alarcon, E.: 'Scalability analysis of simo non-radiative resonant wireless power transfer systems based on circuit models', *IEEE Transactions on Circuits and Systems I: Regular Papers*, 2015, **62**, (10), pp. 2574–2583
- 4 Ku, M.L., Han, Y., Lai, H.Q., Chen, Y., Liu, K.J.R.: 'Power waveforming: Wireless power transfer beyond time reversal', *IEEE Transactions on Signal Processing*, 2016, **64**, (22), pp. 5819–5834
- 5 Huang, Y., Clerckx, B.: 'Large-scale multiantenna multisine wireless power transfer', *IEEE Transactions on Signal Processing*, 2017, **65**, (21), pp. 5812–5827
- 6 Hu, Z., Yuan, C., Gao, F.: 'Maximizing harvested energy for full-duplex swipt system with power splitting', *IEEE Access*, 2017, **5**, pp. 24975–24987
- 7 Sun, H., Lin, H., Zhu, F., Gao, F.: 'Magnetic resonant beamforming for secured wireless power transfer', *IEEE Signal Processing Letters*, 2017, **24**, (8), pp. 1173–1177
- 8 Huang, S., Li, Z., Lu, K.: 'Frequency splitting suppression method for four-coil wireless power transfer system', *IET Power Electronics*, 2016, **9**, (15), pp. 2859–2864
- 9 Junussov, A., Bagheri, M., Lu, M. 'Analysis of magnetically coupled resonator and four-coil wireless charging systems for ev'. In: 2017 International Conference on Sustainable Energy Engineering and Application (ICSEEA). (, 2017, pp. 1–7
- 10 Sultanbek, A., Khassenov, A., Kanapyanov, Y., Kenzhegaliyeva, M., Bagheri, M. 'Intelligent wireless charging station for electric vehicles'. In: 2017 International Siberian Conference on Control and Communications (SIBCON). (, 2017, pp. 1–6
- 11 Moon, S., Moon, G.W.: 'Wireless power transfer system with an asymmetric four-coil resonator for electric vehicle battery chargers', *IEEE Transactions on Power Electronics*, 2016, **31**, (10), pp. 6844–6854
- 12 Kiani, M., Jow, U.M., Ghovanloo, M.: 'Design and optimization of a 3-coil inductive link for efficient wireless power transmission', *IEEE Transactions on Biomedical Circuits and Systems*, 2011, **5**, (6), pp. 579–591
- 13 Li, Y., Xu, Q., Lin, T., Hu, J., He, Z., Mai, R.: 'Analysis and design of load-independent output current or output voltage of a three-coil wireless power transfer system', *IEEE Transactions on Transportation Electrification*, 2018, pp. 1–1
- 14 Stielau, O.H., Covic, G.A. 'Design of loosely coupled inductive power transfer systems'. In: Proc. International Conference on Power System Technology, 2000. Proceedings. PowerCon 2000. vol. 1. (, 2000, pp. 85–90 vol.1
- 15 Lee, C.K., Zhong, W.X. 'Wireless power transfer systems for electric vehicles'. In: Energy Systems for Electric and Hybrid Vehicles. Transport. (Institution of Engineering and Technology, 2016, pp. 261–288
- 16 Feng, P., Xu, T., Li, Y., Zhang, X., Gao, X., Dong, Z., et al. 'The modeling analysis of wireless power transmission under the basic topology structure'. In: 2017 International Conference on Computer Systems, Electronics and Control (ICCSEC). (, 2017, pp. 362–367
- 17 Wang, S., Chen, J., Hu, Z., Rong, C., Liu, M.: 'Optimisation design for series-series dynamic wpt system maintaining stable transfer power', *IET Power Electronics*, 2017, **10**, (9), pp. 987–995

- 18 Qi, P., Xu, J., Yi, F., Zhang, Y., Wang, P., Feng, L., et al. 'The characteristic analysis of magnetically coupled resonant wireless power transmission based on ss compensation structure'. In: 2017 First International Conference on Electronics Instrumentation Information Systems (EIIS). (, 2017, pp. 1–4
- 19 Wang, C.S., Covic, G.A., Stielau, O.H.: 'Power transfer capability and bifurcation phenomena of loosely coupled inductive power transfer systems', *IEEE Transactions on Industrial Electronics*, 2004, **51**, (1), pp. 148–157
- 20 Rakhimbay, A., Bagheri, M., Lu, M. 'A simulation study on four different compensation topologies in ev wireless charging'. In: 2017 International Conference on Sustainable Energy Engineering and Application (ICSEEA). (, 2017, pp. 66–73
- 21 Aditya, K., Williamson, S.S. 'Design considerations for loosely coupled inductive power transfer (ipt) system for electric vehicle battery charging - a comprehensive review'. In: 2014 IEEE Transportation Electrification Conference and Expo (ITEC). (, 2014, pp. 1–6
- 22 Wu, H.H., Gilchrist, A., Sealy, K., Israelsen, P., Muhs, J. 'Design of symmetric voltage cancellation control for lcl converters in inductive power transfer systems'. In: Proc. 2011 IEEE International Electric Machines Drives Conference (IEMDC). (, 2011, pp. 866–871
- 23 Liu, F., Zhang, Y., Chen, K., Zhao, Z., Yuan, L. 'A comparative study of load characteristics of resonance types in wireless transmission systems'. In: Proc. 2016 Asia-Pacific International Symposium on Electromagnetic Compatibility (APEMC). vol. 01. (, 2016, pp. 203–206
- 24 Zhou, S., Mi, C.C.: 'Multi-parallelized lcc reactive power compensation networks and their tuning method for electric vehicle dynamic wireless charging', *IEEE Transactions on Industrial Electronics*, 2016, **63**, (10), pp. 6546–6556
- 25 Wu, M., Chen, X., Mu, X., Pan, Z., Liu, H., Zhou, Y. 'Design of a lifting transportation prototype with the wireless power transmission technology'. In: 2017 36th Chinese Control Conference (CCC). (, 2017, pp. 10291–10297
- 26 Zhou, S., Zhu, C., Yu, C., Chan, C.C. 'A multiplexing lcl module using individual transmitters for dynamic wireless charging of electric vehicles'. In: 2017 IEEE Energy Conversion Congress and Exposition (ECCE). (, 2017, pp. 2728–2733
- 27 Esteban, B., Sid-Ahmed, M., Kar, N.C.: 'A comparative study of power supply architectures in wireless ev charging systems', *IEEE Transactions on Power Electronics*, 2015, **30**, (11), pp. 6408–6422
- 28 Wu, M., Chen, X., Mu, X., Pan, Z., Liu, H., Zhou, Y. 'Design of a lifting transportation prototype with the wireless power transmission technology'. In: 2017 36th Chinese Control Conference (CCC). (, 2017, pp. 10291–10297
- 29 Su, Y., Tang, C., Wu, S., Sun, Y. 'Research of lcl resonant inverter in wireless power transfer system'. In: 2006 International Conference on Power System Technology. (, 2006, pp. 1–6
- 30 Cai, C., Wang, J., Fang, Z., Zhang, P., Hu, M., Zhang, J., et al.: 'Design and optimization of load-independent magnetic resonant wireless charging system for electric vehicles', *IEEE Access*, 2018, **PP**, (99), pp. 1–1
- 31 Li, W., Zhao, H., Li, S., Deng, J., Kan, T., Mi, C.C.: 'Integrated LCC compensation topology for wireless charger in electric and plug-in electric vehicles', *IEEE Transactions on Industrial Electronics*, 2015, **62**, (7), pp. 4215–4225
- 32 Kan, T., Nguyen, T.D., Wjite, J.C., Malhan, R.K., Mi, C.: 'A new integration method for an electric vehicle wireless charging system using lcc compensation topology', *IEEE Transactions on Power Electronics*, 2016, **PP**, (99), pp. 1–1
- 33 Rasekh, N., Kavianpour, J., Mirsalim, M.: 'A novel integration method for a bipolar receiver pad using lcc compensation topology for wireless power transfer', *IEEE Transactions on Vehicular Technology*, 2018, **67**, (8), pp. 7419–7428
- 34 Li, Y., Lin, T., Mai, R., Huang, L., He, Z.: 'Compact double-sided decoupled coils-based wpt systems for high-power applications: Analysis, design, and experimental verification', *IEEE Transactions on Transportation Electrification*, 2018, **4**, (1), pp. 64–75
- 35 Lu, F., Zhang, H., Hofmann, H., Mi, C.C.: 'A dynamic charging system with reduced output power pulsation for electric vehicles', *IEEE Transactions on Industrial Electronics*, 2016, **63**, (10), pp. 6580–6590
- 36 Li, W., Zhao, H., Deng, J., Li, S., Mi, C.C.: 'Comparison study on ss and double-sided lcc compensation topologies for ev/phev wireless chargers', *IEEE Transactions on Vehicular Technology*, 2016, **65**, (6), pp. 4429–4439
- 37 Wang, Y., Yao, Y., Liu, X., Xu, D., Cai, L.: 'An lcl-s compensation topology and coil design technique for wireless power transfer', *IEEE Transactions on Power Electronics*, 2018, **33**, (3), pp. 2007–2025
- 38 Yao, Y., Wang, Y., Liu, X., Xu, D.: 'Analysis, design, and optimization of lcc compensation topology with excellent load-independent voltage output for inductive power transfer', *IEEE Transactions on Transportation Electrification*, 2018, **4**, (3), pp. 767–777
- 39 Ong, A., Sampath, J.P.K., Beng, G.F.H., YenKheng, T., Vilathgamuwa, D.M., Bac, N.X. 'Analysis of impedance matched circuit for wireless power transfer'. In: IECON 2014 - 40th Annual Conference of the IEEE Industrial Electronics Society. (, 2014, pp. 2965–2970
- 40 Byeon, J., Kang, M., Kim, M., Joo, D.M., Lee, B.K. 'Hybrid control of inductive power transfer charger for electric vehicles using lcl-s resonant network in limited operating frequency range'. In: 2016 IEEE Energy Conversion Congress and Exposition (ECCE). (, 2016, pp. 1–6
- 41 Yang, S., Sun, P., Wu, X., Shao, Y., Sun, J. 'Parameter design and verification of inductive contactless power transfer system based on double-sided lcl resonance'. In: 2018 13th IEEE Conference on Industrial Electronics and Applications (ICIEA). (, 2018, pp. 2393–2398
- 42 'Qi wireless charging standard'. (, . <http://www.radio-electronics.com/info/power-management/wireless-inductive-battery-charging/qi-wireless-charging-standard.php>
- 43 GOLDEN, P. 'Qi wireless charging everywhere? it's coming'. (, . <https://www.wirelesspowerconsortium.com/blog/280/qi-wireless-charging-everywhere-its-coming>

- 44 'A4wp wireless charging'. (. . . <http://www.radio-electronics.com/info/power-management/wireless-inductive-battery-charging/a4wp-wireless-charging.php>)
- 45 BLANCO, S.. 'Sae now has a wireless charging standard:j2954'. (. . . <https://www.autoblog.com/2016/05/26/sae-now-has-a-wireless-charging-standard-j2954/>)
- 46 (. . . http://www.sae.org/smartgrid/sae-j2954-status_1-2012.pdf)
- 47 Warrington, C.. 'Charging on the go'. (. . . <https://ieccetech.org/index.php/Technology-Focus/2017-03/Charging-on-the-go>)
- 48 'Iec releases iec 62827-1:2016, standard for wireless power transfer'. (. . . <https://incompliancemag.com/iec-releases-iec-62827-12016-standard-for-wireless-power-transfer/>)
- 49 Traube, J., Lu, F., Maksimovic, D., Mossoba, J., Kromer, M., Faill, P., et al.: 'Mitigation of solar irradiance intermittency in photovoltaic power systems with integrated electric-vehicle charging functionality', *IEEE Transactions on Power Electronics*, 2013, **28**, (6), pp. 3058–3067
- 50 'The global electric-vehicle market is amped up and on the rise'. (. . . <https://www.mckinsey.com>)
- 51 Li, S., Mi, C.C.: 'Wireless power transfer for electric vehicle applications', *IEEE Journal of Emerging and Selected Topics in Power Electronics*, 2015, **3**, (1), pp. 4–17
- 52 'Electric vehicle telematics and charging control'. (. . . <https://www.fleetcarma.com>)
- 53 Nissan. 'Leaf'. (. . . <https://www.nissan.co.uk/vehicles/newvehicles/leaf.html>, accessed June 2017)
- 54 News, E.V.. 'Electric vehicle news'. (. . . <http://www.electricvehiclenews.com/2014/05/volvo-to-develop-electric-roads-for.html>, accessed Apr. 2017)
- 55 'Government to investigate wireless charging for electric cars'. (. . . <https://www.autoexpress.co.uk/car-news/electric-cars/100194/government-to-investigate-wireless-charging-for-electric-cars>)
- 56 Liu, C., Chau, K.T., Wu, D., Gao, S.: 'Opportunities and challenges of vehicle-to-home, vehicle-to-vehicle, and vehicle-to-grid technologies', *Proceedings of the IEEE*, 2013, **101**, (11), pp. 2409–2427
- 57 'Honda unveils two-way wireless v2g energy management system'. (. . . <https://chargedevs.com/newswire/honda-unveils-two-way-wireless-v2g-energy/-management-system/>)
- 58 Hui, S.Y.R., Zhong, W., Lee, C.K.: 'A critical review of recent progress in mid-range wireless power transfer', *IEEE Transactions on Power Electronics*, 2014, **29**, (9), pp. 4500–4511
- 59 Theodoropoulos, T., Damousis, Y., Amditis, A. 'A load balancing control algorithm for ev static and dynamic wireless charging'. In: 2015 IEEE 81st Vehicular Technology Conference (VTC Spring). (. . . 2015, pp. 1–5)
- 60 Esteban, B., Sid.Ahmed, M., Kar, N.C.: 'A comparative study of power supply architectures in wireless ev charging systems', *IEEE Transactions on Power Electronics*, 2015, **30**, (11), pp. 6408–6422
- 61 Hsieh, Y., Lin, Z., Chen, M., Hsieh, H., Liu, Y., Chiu, H.: 'High-efficiency wireless power transfer system for electric vehicle applications', *IEEE Transactions on Circuits and Systems II: Express Briefs*, 2017, **64**, (8), pp. 942–946
- 62 Kan, T., Nguyen, T., White, J.C., Malhan, R.K., Mi, C.C.: 'A new integration method for an electric vehicle wireless charging system using lcc compensation topology: Analysis and design', *IEEE Transactions on Power Electronics*, 2017, **32**, (2), pp. 1638–1650
- 63 Cai, C., Wang, J., Fang, Z., Zhang, P., Hu, M., Zhang, J., et al.: 'Design and optimization of load-independent magnetic resonant wireless charging system for electric vehicles', *IEEE Access*, 2018, **6**, pp. 17264–17274
- 64 Chung, Y.D., Lee, C.Y., Kang, H., Park, Y.G.: 'Design considerations of superconducting wireless power transfer for electric vehicle at different inserted resonators', *IEEE Transactions on Applied Superconductivity*, 2016, **26**, (4), pp. 1–5
- 65 Zhang, W., White, J.C., Abraham, A.M., Mi, C.C.: 'Loosely coupled transformer structure and interoperability study for ev wireless charging systems', *IEEE Transactions on Power Electronics*, 2015, **30**, (11), pp. 6356–6367
- 66 Kim, J., Son, H., Kim, D., Kim, K., Park, Y. 'Efficiency of magnetic resonance wpt with two off-axis self-resonators'. In: 2011 IEEE MTT-S International Microwave Workshop Series on Innovative Wireless Power Transmission: Technologies, Systems, and Applications. (. . . 2011, pp. 127–130)
- 67 Kim, H., Song, C., Kim, D., Jung, D.H., Kim, I., Kim, Y., et al.: 'Coil design and measurements of automotive magnetic resonant wireless charging system for high-efficiency and low magnetic field leakage', *IEEE Transactions on Microwave Theory and Techniques*, 2016, **64**, (2), pp. 383–400
- 68 Mou, X., Sun, H. 'Wireless power transfer: Survey and roadmap'. In: Proc. of 81st IEEE Vehicular Technology Conference. (. . . 2015, pp. 1–5)
- 69 Yang, G., Zhu, C., Song, K., Liu, K., Lu, R., Wei, G. 'Power stability optimization method of wireless power transfer system against wide misalignment'. In: 2017 IEEE Transportation Electrification Conference and Expo, Asia-Pacific (ITEC Asia-Pacific). (. . . 2017, pp. 1–6)
- 70 Dang, Z., Qahouq, J.: 'Modeling and investigation of magnetic resonance coupled wireless power transfer system with lateral misalignment', *Proc 29th Annual IEEE Applied Power Electronics Conference and Exposition (APEC)*, 2014, pp. 1313–1322
- 71 Fotopoulou, K., Flynn, B.: 'Wireless power transfer in loosely coupled links', *Proc IEEE Transactions on Magnetics*, 2011, **47**, (2), pp. 413–430
- 72 Fernandes, R.C., de Oliveira, A.: 'Iterative design method of weakly coupled magnetic elements for inductive power transfer', *Proc Brazilian Power Electronics Conference (COBEP)*, 2013, pp. 1088–1093
- 73 Jegadeesan, R., and. 'Overcoming coil misalignment using magnetic fields of induced currents in wireless power transmission'. In: 2012 IEEE/MTT-S International Microwave Symposium Digest. (. . . 2012, pp. 1–3)
- 74 Luo, Z., Wei, X. 'Mutual inductance analysis of planar coils with misalignment for wireless power transfer systems in electric vehicle'. In: 2016 IEEE Vehicle Power and Propulsion Conference (VPPC). (. . . 2016, pp. 1–6)
- 75 H.Hoang, Y.C., Bien, F.: 'Efficiency improvement for magnetic resonance based wireless power transfer with axial-misalignment', *Electronics Letters*, 2012, **48**, (6), pp. 339–341
- 76 Miwa, K., Kaneda, J., Kikuma, N., Hirayama, H., Sakakibara, K. 'Consideration of use of arrayed transmitting coils in wireless power transfer with magnetically coupled resonance'. In: 2012 International Symposium on Antennas and Propagation (ISAP). (. . . 2012, pp. 451–454)
- 77 Mori, K., Lim, H., Iguchi, S., Ishida, K., Takamiya, M., Sakurai, T.: 'Positioning-free resonant wireless power transmission sheet with staggered repeater coil array (sca)'. *IEEE Antennas and Wireless Propagation Letters*, 2012, **11**, pp. 1710–1713
- 78 Miwa, K., Mori, H., Kikuma, N., Hirayama, H., Sakakibara, K. 'A consideration of efficiency improvement of transmitting coil array in wireless power transfer with magnetically coupled resonance'. In: 2013 IEEE Wireless Power Transfer (WPT). (. . . 2013, pp. 13–16)
- 79 Gao, Y., Duan, C., Oliveira, A.A., Ginart, A., Farley, K.B., Tse, Z.T.H.: '3-d coil positioning based on magnetic sensing for wireless ev charging', *IEEE Transactions on Transportation Electrification*, 2017, **3**, (3), pp. 578–588
- 80 Zhao, L., Thrimawithana, D.J., Madawala, U.K.: 'Hybrid bidirectional wireless ev charging system tolerant to pad misalignment', *IEEE Transactions on Industrial Electronics*, 2017, **64**, (9), pp. 7079–7086
- 81 Li, Y., Li, X., Peng, F., Zhang, H., Guo, W., Zhu, W., et al. 'Wireless energy transfer system based on high q flexible planar-litz mems coils'. In: Proc. 2013 8th IEEE International Conference on Nano/Micro Engineered and Molecular Systems (NEMS). (. . . 2013, pp. 837–840)
- 82 Mizuno, T., Yachi, S., Kamiya, A., Yamamoto, D.: 'Improvement in efficiency of wireless power transfer of magnetic resonant coupling using magnetoplated wire', *IEEE Transactions on Magnetics*, 2011, **47**, (10), pp. 4445–4448
- 83 Sampath, J.P.K., Alphones, A., Kenneth, L.Y.Y., Vilathgamuwa, D.M. 'Analysis on normalized distance and scalability in designing wireless power transfer'. In: Proc. 2015 IEEE PELS Workshop on Emerging Technologies: Wireless Power (WoW). (. . . 2015, pp. 1–6)
- 84 Kurschner, D., Rathge, C., Jumar, U.: 'Design methodology for high efficient inductive power transfer systems with high coil positioning flexibility', *IEEE Transactions on Industrial Electronics*, 2013, **60**, (1), pp. 372–381
- 85 Flynn, B.W., Fotopoulou, K.: 'Rectifying loose coils: Wireless power transfer in loosely coupled inductive links with lateral and angular misalignment', *IEEE Microwave Magazine*, 2013, **14**, (2), pp. 48–54
- 86 Xianjin, S., Guoqiang, L., Yanhong, L., Chao, Z., Xiaoyu, X. 'Analyses and experiments of field-circuit coupling equations for wireless power transfer using solenoidal coils'. In: Proc. 2015 IEEE International Wireless Symposium (IWS). (. . . 2015, pp. 1–4)
- 87 Feenaghty, M., Dahle, R. 'A compact and high quality factor archimedean coil geometry for wireless power transfer'. In: 2016 IEEE Wireless Power Transfer Conference (WPTC). (. . . 2016, pp. 1–3)
- 88 Pantic, Z., Lukic, S.: 'Computationally-efficient, generalized expressions for the proximity-effect in multi-layer, multi-turn tubular coils for wireless power transfer systems', *IEEE Transactions on Magnetics*, 2013, **49**, (11), pp. 5404–5416
- 89 Nguyen, M.Q., Hughes, Z., Woods, P., Seo, Y.S., Rao, S., Chiao, J.C.: 'Field distribution models of spiral coil for misalignment analysis in wireless power transfer systems', *IEEE Transactions on Microwave Theory and Techniques*, 2014, **62**, (4), pp. 920–930
- 90 Limited, U.F. 'Ev city casebook 50 big ideas shaping the future of electric mobility'. (. . . <http://urbanforesight.org/projects/case-studies/detail/ev-city-casebook-50-big-ideas-shaping-future-electric-mobility>, accessed Mar. 2017)
- 91 Primove. 'Primove website'. (. . . <http://primove.bombardier.com/media/publications.html/>, accessed April 2017.
- 92 Theodoropoulos, T., Damousis, Y., Amditis, A. 'A load balancing control algorithm for ev static and dynamic wireless charging'. In: 2015 IEEE 81st Vehicular Technology Conference (VTC Spring). (. . . 2015, pp. 1–5)
- 93 Theodoropoulos, T., Amditis, A., Sall'Åan, J., Bludszweit, H., Berseneff, B., Guglielmi, P., et al. 'Impact of dynamic ev wireless charging on the grid'. In: 2014 IEEE International Electric Vehicle Conference (IEVC). (. . . 2014, pp. 1–7)
- 94 Naberezhnykh, D., Reed, N., Ognissanto, F., Theodoropoulos, T., Bludszweit, H. 'Operational requirements for dynamic wireless power transfer systems for electric vehicles'. In: 2014 IEEE International Electric Vehicle Conference (IEVC). (. . . 2014, pp. 1–8)
- 95 Cui, S., Wang, Z., Han, S., Zhu, C., Chan, C.C.: 'Analysis and design of multiphase receiver with reduction of output fluctuation for ev dynamic wireless charging system', *IEEE Transactions on Power Electronics*, 2018, pp. 1–1
- 96 Wang, Y., Hu, X., Yao, Y., Liu, X., Xu, D., Cai, L., et al. 'A dynamic wireless power transfer system with parallel transmitters'. In: 2017 IEEE Transportation Electrification Conference and Expo, Asia-Pacific (ITEC Asia-Pacific). (. . . 2017, pp. 1–6)
- 97 Zhang, Z., Jia, B., Pang, H., Liu, C. 'Comparative analysis and optimization of dynamic charging coils for roadway-powered electric vehicles'. In: 2017 IEEE International Magnetics Conference (INTERMAG). (. . . 2017, pp. 1–1

- 98 Miller, J.M., Onar, O.C., White, C., Campbell, S., Coomer, C., Seiber, L., et al.: 'Demonstrating dynamic wireless charging of an electric vehicle: The benefit of electrochemical capacitor smoothing', *IEEE Power Electronics Magazine*, 2014, **1**, (1), pp. 12–24
- 99 Hariri, A., Elsayed, A., Mohammed, O.A.: 'An integrated characterization model and multiobjective optimization for the design of an ev charger's circular wireless power transfer pads', *IEEE Transactions on Magnetics*, 2017, **53**, (6), pp. 1–4
- 100 Budhia, M., Covic, G., Boys, J.: 'A new ipt magnetic coupler for electric vehicle charging systems'. In: Proc. IECON 2010 - 36th Annual Conference on IEEE Industrial Electronics Society. (, 2010. pp. 2487–2492
- 101 Choi, S.Y., Gu, B.W., Jeong, S.Y., Rim, C.T.: 'Advances in wireless power transfer systems for roadway-powered electric vehicles', *IEEE Journal of Emerging and Selected Topics in Power Electronics*, 2015, **3**, (1), pp. 18–36
- 102 Budhia, M., Boys, J.T., Covic, G.A., Huang, C.: 'Development of a single-sided flux magnetic coupler for electric vehicle ipt charging systems', *IEEE Transactions on Industrial Electronics*, 2013, **60**, (1), pp. 318–328
- 103 Covic, G.A., Kissin, M.L.G., Kacprzak, D., Clausen, N., Hao, H.: 'A bipolar primary pad topology for ev stationary charging and highway power by inductive coupling'. In: Proc. 2011 IEEE Energy Conversion Congress and Exposition. (, 2011. pp. 1832–1838
- 104 Nguyen, T.D., Li, S., Li, W., Mi, C.C.: 'Feasibility study on bipolar pads for efficient wireless power chargers'. In: Proc. 2014 IEEE Applied Power Electronics Conference and Exposition - APEC 2014. (, 2014. pp. 1676–1682
- 105 Zhang, Z., Pang, H., Lee, C.H.T., Xu, X., Wei, X., Wang, J.: 'Comparative analysis and optimization of dynamic charging coils for roadway-powered electric vehicles', *IEEE Transactions on Magnetics*, 2017, **53**, (11), pp. 1–6
- 106 Xiang, L., Sun, Y., Tang, C., Dai, X., Jiang, C.: 'Design of crossed dd coil for dynamic wireless charging of electric vehicles'. In: 2017 IEEE PELS Workshop on Emerging Technologies: Wireless Power Transfer (WoW). (, 2017. pp. 1–5
- 107 Bertoluzzo, M., Buja, G., Dashora, H.K.: 'Design of dwc system track with unequal dd coil set', *IEEE Transactions on Transportation Electrification*, 2017, **3**, (2), pp. 380–391
- 108 Chen, Z., Jing, W., Huang, X., Tan, L., Chen, C., Wang, W.: 'A promoted design for primary coil in roadway-powered system', *IEEE Transactions on Magnetics*, 2015, **51**, (11), pp. 1–4
- 109 Hwang, I., Jang, Y.J., Ko, Y.D., Lee, M.S.: 'System optimization for dynamic wireless charging electric vehicles operating in a multiple-route environment', *IEEE Transactions on Intelligent Transportation Systems*, 2017, pp. 1–18
- 110 Shin, S., Shin, J., Kim, Y., Lee, S., Song, B., Jung, G., et al.: 'Hybrid inverter segmentation control for online electric vehicle'. In: Proc. 2012 IEEE International Electric Vehicle Conference. (, 2012. pp. 1–6
- 111 Beh, H.Z.Z., Covic, G.A., Boys, J.T.: 'Wireless fleet charging system for electric bicycles', *IEEE Journal of Emerging and Selected Topics in Power Electronics*, 2015, **3**, (1), pp. 75–86
- 112 Nagendra, G.R., Boys, J.T., Covic, G.A., Riar, B.S., Sondhi, A.: 'Design of a double coupled ipt ev highway'. In: Proc. IECON 2013 - 39th Annual Conference of the IEEE Industrial Electronics Society. (, 2013. pp. 4606–4611
- 113 Deng, Q., Liu, J., Czarkowski, D., Bojarski, M., Chen, J., Hu, W., et al.: 'Edge position detection of on-line charged vehicles with segmental wireless power supply', *IEEE Transactions on Vehicular Technology*, 2017, **66**, (5), pp. 3610–3621
- 114 Lee, S., Huh, J., Park, C., Choi, N.S., Cho, G.H., Rim, C.T.: 'On-line electric vehicle using inductive power transfer system'. In: Proc. 2010 IEEE Energy Conversion Congress and Exposition. (, 2010. pp. 1598–1601
- 115 Huh, J., Lee, S.W., Lee, W.Y., Cho, G.H., Rim, C.T.: 'Narrow-width inductive power transfer system for online electrical vehicles', *IEEE Transactions on Power Electronics*, 2011, **26**, (12), pp. 3666–3679
- 116 Park, C., Lee, S., Jeong, S.Y., Cho, G.H., Rim, C.T.: 'Uniform power i-type inductive power transfer system with dq-power supply rails for on-line electric vehicles', *IEEE Transactions on Power Electronics*, 2015, **30**, (11), pp. 6446–6455
- 117 Choi, S.Y., Jeong, S.Y., Gu, B.W., Lim, G.C., Rim, C.T.: 'Ultraslim s-type power supply rails for roadway-powered electric vehicles', *IEEE Transactions on Power Electronics*, 2015, **30**, (11), pp. 6456–6468
- 118 Mi, C.C., Buja, G., Choi, S.Y., Rim, C.T.: 'Modern advances in wireless power transfer systems for roadway powered electric vehicles', *IEEE Transactions on Industrial Electronics*, 2016, **63**, (10), pp. 6533–6545
- 119 Thai, V.X., Choi, S.Y., Choi, B.H., Kim, J.H., Rim, C.T.: 'Coreless power supply rails compatible with both stationary and dynamic charging of electric vehicles'. In: Proc. 2015 IEEE 2nd International Future Energy Electronics Conference (IFEEC). (, 2015. pp. 1–5
- 120 Chen, L., Nagendra, G.R., Boys, J.T., Covic, G.A.: 'Double-coupled systems for ipt roadway applications', *IEEE Journal of Emerging and Selected Topics in Power Electronics*, 2015, **3**, (1), pp. 37–49